(77)

A Renormalization Approach to Diffusion-Limited Aggregation

by

Matthew B. Hastings

Submitted to the Department of Physics
in partial fulfillment of the requirements for the degree of

Doctor of Philosophy in Physics

at the

MASSACHUSETTS INSTITUTE OF TECHNOLOGY

July 1997
[September 1997]

Author .....
Department of Physics
July 10, 1997

Certified by .....
Leonid S. Levitov
Associate Professor
Thesis Supervisor

Accepted by .....
George F. Koster
Chairman, Departmental Committee on Graduate Students

A Renormalization Approach to Diffusion-Limited Aggregation

by

Matthew B. Hastings

Submitted to the Department of Physics
on July 10, 1997, in partial fulfillment of the
requirements for the degree of
Doctor of Philosophy in Physics

Abstract

Diffusion-limited aggregation (DLA) is a growth model formulated in terms of random walkers. An alternative formulation of DLA is presented based on conformal mappings in two dimensions. As far as one can tell, the two descriptions are equivalent.

An analytical renormalization group treatment is presented of this model. The fractal dimension of DLA is computed to be $2 - 1/2 + 1/5 = 1.7$. Higher multifractal exponents are also calculated and found in agreement with numerical results. It may be possible to use this technique to describe the dielectric breakdown model as well, which is given by different parameter values.

Thesis Supervisor: Leonid S. Levitov
Title: Associate Professor

Acknowledgments

First, I would like to thank my advisor, Leonid Levitov, who suggested the problem of Laplacian growth, invented the first $\alpha = 0$ version of the conformal model, and provided much useful advice.

I would also like to thank several other physicists for my education. Frank Firk taught freshman physics at Yale at a level beyond that of any other course I have taken. I would also like to thank Doug Stone at Yale, with whom I did research while I was an undergrad. Of the many people at MIT, I would particularly like to thank Jens Siewert, Christopher Mudry, and Patrick Lee.

Special thanks to: Adam Young, drums, bass, guitar, vocals; Alex Babin, guitar, vocals; Joe Alia, alto saxophone; Mike Croft, guitar; Larry Coar, drums (lots of drums) and percussion (lots of percussion); Rich Vigdor, guitar; John LaMaster, guitar, vocals; Han-Mi Park, vocals; Toby Turner, guitar, vocals; Jim Titus, guitar, vocals. Of these people, I would especially like to thank Adam Young, who taught me how to play bass, and Larry Coar, drummer extraordinaire. Thanks to *Bleach*, *The Idea*, and *Lid*. Thanks to Mandy and Mike and the rest of the Titus family.

Thanks to Sleight and Trent.

Thanks to Jim McCormack, and all the other skiers. There are no rules above 10,000 feet.

Thanks to the Pour House. Thanks, all!

Contents

List of Figures

Chapter 1

Introduction and Notation

1.1 Introduction

There are many physical problems in nature in which fractal structures appear[1]. Many models have been invented, employing simple growth rules to produce structures that mimic those of nature[2, 3, 4]. The model of diffusion-limited aggregation (DLA) [5] is one of the most famous of these. There have been intensive numerical studies of this model and it appears to defy most standard analytical approaches.

In this thesis [1], a new formulation of DLA is presented, together with a renormalization group approach that yields analytical values for fractal and multifractal exponents. In this introduction, we will first review the concept of fractality, as well as indicate the use of renormalization group procedures in attacking growth problems. Next, the DLA model will be defined and some explanation will be given as to why DLA is so complicated a problem. Previous work on DLA will be briefly reviewed, and then the RG and other analytical work of this paper will be outlined.

[1] With the exception of sections (1.1-1.4), the first paragraph of section (1.5), section (2.2), section (5.2), Appendix B, and Appendix C, this work is Copyright The American Physical Society 1997. All rights reserved. Except as provided under U. S. copyright law, this work may not be reproduced, resold, distributed or modified without the express permission of The American Physical Society. The archival version of this work was published in Physical Review E, Volume 55, page 135.

1.2 Fractal Geometry

Some of the basic properties of fractal sets were investigated early in this century by Hausdorff and Besicovitch[6, 7]. Originally these sets were regarded as "monsters"; it was the work of Mandelbrot, though, that helped show how common such structures are in nature.

The basic property of a fractal is scale-invariance. Smaller portions of the fractal set look similar to the whole set. One finds this in many situations in nature. A classic example is that the outline of a small stretch of beach is similar to the outline of an entire coastline. Similarly, one may find that small branches on a tree look similar to large branches, just scaled down in size. In the DLA problem, one finds many arms extending from the center of the cluster, each with smaller arms coming off of it, with some self-similarity as one looks at smaller and smaller arms.

One of the simplest self-similar sets is the path of a random walker. Consider the path that a random walker takes in a time t. If one scales this path that the walker takes by a factor $\sqrt{n}$, one has a path that is equivalent to that of a random walker moving for a time nt. Equivalently, one can say that any small segment of the path has the same statistical properties as the whole path, after rescaling by some amount.

This example will help to introduce the concept of dimension. Consider the path of such a random walker in a three-dimensional space. The walker's path is defined by a line, but this line is very complicated. Let us calculate the length of this line. According to the typical definition of a random walk the mean-square distance traveled in a time t is proportional to the square root of t. Therefore, the length of the path of a random walker moving for a time t must be at least the distance traveled and so the length of the path must then be at least the square root of t. However, by dividing the time t into n time intervals of length t/n, we find that the length of the past must be at least $n\sqrt{t/n}$. This diverges as $n \to \infty$. The path of the random walker is thus infinitely long even for a finite length of time. This is a hint that the path of a random walker is somehow "bigger" than a one-dimensional line segment. In fact, according to the box-counting definition of dimension outlined below, the

random walk has fractal dimension two, although it has topological dimension one[8]. In more general situations, we may find objects with non-integer dimension.

One may define the dimension of a set embedded in a D-dimensional space in many ways. The topological dimension is defined by considering all open coverings of the set with balls of radius less than ϵ. If a set has topological dimension d, then this means that, for any ϵ, one can find a covering such that no more than $d+1$ balls intersect at any point, but that one cannot find a covering such that no more than d balls intersect at any point. This definition of dimension always yields an integer number, and is *not* suited to the problem of describing fractal structures. Instead, we seek another definition of dimension. The box-counting dimension of a set proceeds as follows: place a grid on the D-dimensional embedding space with grid spacing ϵ. Consider the number of grid squares which contain a point of the set. As the size of the grid tends to zero, if one finds that this number varies in a power law fashion with ϵ, than the fractal dimension of the set is said to be this power. This is an example of what we may call a mass versus radius relation. The mass of the set is the total number of grid squares is occupies. The radius is the size of the grid square. Such relations are familiar from elementary geometry; for example, the area of the square is the square of the length of the sides, while the volume of a cube is the cube of the length of the sides.

For DLA, one finds that the fractal dimension of the growing cluster is approximately 1.71 when the simulation is performed in two dimensional space. The fractal dimension is the single most important number to calculate for a growth problem such as DLA. It characterizes the structure of the set, as well as providing information on growth rate.

In any fractal-like structure found in nature or generated in a simulation, one would not expect such a power law to hold for arbitrarily small ϵ. Instead, there is a scaling region in which the power law holds. For ϵ too small, one begins to go below some microscopic cutoff of the problem, while for ϵ too large, one begins to consider ϵ of the order of the size of the set itself. If we consider the random walker again, although a smaller segment of the path is equivalent to a larger segment of the path,

eventually, at some microscopic scale, this does not hold. For example, in a random walker problem arising from Brownian motion, at an atomic length scale the particles follow straight lines between collisions with other atoms.

There are many other definitions of fractal dimension and one would expect them all to agree if the set being considered is indeed a fractal. One of the most important other definitions is the radius of gyration definition. In a typical growth problem, the microscopic cutoff stays fixed while the cluster grows. This means that over time the scaling region for the box-counting dimension increases. In most growth problems, the mass goes linearly with the time. The means that if one finds a relation like $R \propto t^{1/d}$ where R is the radius of the object and t is the time, perhaps measured in number of growth steps, then one may consider d to be the dimension of the object. The only problem is how to measure the radius. In the limit of infinitely long time, all definitions of radius will give the same result for the exponent. The radius of gyration technique defines the radius to be the radius of gyration of the object (square root of the sum of squares of radii, where the sum is taken over each walker added to the cluster) and is chosen because it is numerically more accurate than other definitions of radius.

1.3 Renormalization Group Approaches

The renormalization group was developed for statistical mechanics problems near a second order phase transition where the system becomes scale invariant. It would seem natural to try to use RG-type procedures to deal with fractal problems. Unfortunately, there are many complications. In statistical mechanics, one must tune the problem to a temperature very close to the critical temperature to see scale invariance, while in problems such as the DLA model outlined below or the random walker problem discussed above, there does not appear to be any parameter which must be carefully adjusted to lead to scale invariance. Further, in statistical mechanics, one must simply sum over all configurations, with a weight determined in a trivial fashion by the configuration. In growth problems, one must sum over all configurations with

a weight *determined by the history of the growth.* The fixed-scale transformation is an attempt to define a general method of dealing with growth problems which deals with these difficulties[9]. In this thesis, however, we will use a more conventional RG-type approach instead of a fixed-scale transformation or other approach. One should be aware, though, that these difficulties discussed above will show up in some non-standard features of the RG of this work.

1.4 Definition of DLA

DLA is a model for growth of a cluster, by the accretion of random walkers, simulating problems in nature such as crystal growth or deposition problems, in circumstances in which diffusion is the main factor controlling growth.

The random walkers are released one at a time from infinity and stick when they first contact the cluster. After a walker sticks to the cluster, the next walker is released from infinity. This process gives rise to fractal patterns as a result of competition between branches. If a given branch gets ahead of other branches, it receives a greater flux of walkers and screens the rest of the cluster.

Due to the mathematical equivalence of random walks and potential theory, this definition of the model is equivalent to solving Laplace's equation outside the boundary of the aggregate, setting the potential zero on the aggregate and logarithmically growing at infinity, and picking a point on the surface of the aggregate to add the walker with a probability proportional to the local field strength; this field strength may be thought of as an "electric field". Again, walkers are added one at a time and the field outside the cluster is updated before the next walker is added.

The field strength defines a measure on the surface of the growing cluster. This measure, for a length ds on the surface is equal to $E\,ds$ where E is the electric field. By calculating scaling of the integral over the object of various powers of this measure, one may define multifractal exponents[10, 11, 12].

In one dimension, DLA is obviously a very simple problem: at every stage, the cluster consists of a line segment, and one randomly adds a new object to one or

the other side of the segment at every growth phase. In three or more dimensions, various simple mean-field approaches appear to work very accurately [13, 14]. In two dimensions, however, the situation is more complicated. We may understand this mathematically as follows: the complexity of DLA arises due to strong coupling between different points in the growing cluster. The coupling between two points is a result of the fact that if an incident random walker hits the growing cluster at one point, it sticks, and cannot then continue to the next point. Thus, we may imagine that two points are coupled if there exists a large probability for a random walk to come from infinity, hit one point, and then continue on to the next point. A random walk has fractal dimension two and thus vanishing codimension in two-dimensional space. Therefore, in two space dimensions the random walk couples all points in the growing cluster. In D dimensions, $D > 2$, if a cluster has fractal dimension $d < D$, the random walk couples only to a $d-D+2$ dimensional subset of the cluster (this follows from a general rule that the fractal dimension of the intersection of a d-dimensional set with a d'-dimensional set in a D dimensional space is $d + d' - D$). This implies that in $D > 2$ space dimensions the problem is not strongly coupled.

One might hope that this would make possible a renormalization group approach based on expanding about 3 dimensions, considering this to be the upper critical dimension. Unfortunately, this is not the case. For such an expansion, one would like to expand about a completely uncoupled model, with growth occuring randomly at all sites on the surface, such as the Eden model[2]. However, this is not the situation that the mean-field approaches describe. Also, these approaches are rather heuristic and it is not clear what precisely is the nature of the approximation.

1.5 Review of Previous Work on DLA

There has been much numerical work on DLA in two dimensions, where the fractal dimension has been determined to be 1.71[15]. However there is a complication discussed in [16]. This is that the dimension of DLA is not very well defined: radius of gyration gives 1.71, while the fractal dimension of a cut of DLA at a given radius

is about 0.66. Recalling the rule for the dimension of the intersection of two sets, this would implies that DLA has dimension 1.66. It is interesting that of three recent RG approaches to DLA, the one in this thesis, based on calculating the growth rate, yields 1.7, while the others based on geometrical properties yield numbers closer to 1.66[17, 9]. Mean-field calculations also predict $D = 5/3$[13, 14].

Another important analytic result was the derivation of the electrostatic scaling law, which appears to be obeyed numerically by the aggregates [18, 19]. This law is used as an essential step in the calculation of this thesis.

Recently, another formulation of DLA was proposed, based completely on conformal mappings[20]. A conformal function mapped the unit circle onto the boundary of the aggregate. In this formulation of the problem, the electrostatic scaling law followed almost automatically when considering the behavior of the first Fourier component of the mapping. We investigated numerically the problem of the importance of different Fourier components of the mapping. It appeared that by directly simulating the dynamics of only the first few Fourier components, results could be obtained for short growth periods that were similar to those when the full function was used. This suggested that it might be possible to develop a renormalization theory based on integrating out higher Fourier components, using techniques similar to those used in field theory.

Also, by comparing a picture of the cluster generated by only keeping some small number of terms in the Fourier expansion of the mapping to a picture generated by the full mapping, it appeared that the finite number of terms gave a good description of the boundary of the object. It did not accurately describe the exact microscopic structure of the growth tips, and did not correctly describe the structure of portions of the object far from the growth region, that is, deep in the inside of the object. However, one would expect that the microscopic structure is not too important, and that the description of regions where there is little probability of growth is also not important.

Fig. 1 shows a picture of the cluster that results from the conformal mapping model. The envelope surrounding the cluster was generated from the first 40 terms

of the Fourier series expansion of the mapping used to generate the full cluster.

For longer time periods, more terms in the Fourier series were needed, but this is only to be expected; if only one term were kept in the Fourier series the object would be a circle and would grow with a radius proportional to the square root of time. As more terms are kept, the object can grow faster than the square root of time by changing shape, but for any given number of terms, eventually the growth will be as the square root of time. Therefore, it is expected that in the RG that follows there will be some cutoff in the number of terms kept which increases with the size of the object.

The above discussion is intended to motivate the RG that follows. Most of the discussion is done in more detail in Ref. [20].

Hope, that such a scheme would work, was provided by numerical evidence that the conserved quantities (the moments) of the continuum growth law were very nearly conserved by the random growth process[21]. For the lowest Fourier coefficients, one would expect that the random growth would be close to the average growth determined by the continuum law, while the higher Fourier coefficients would fluctuate more wildly.

1.6 Outline of Thesis

The thesis is divided into several parts. First, the conformal mapping model for DLA is discussed and used to derive continuum equations for growth, essentially equivalent to the Shraiman-Bensimon equation for the Hele-Shaw problem[22]. These equations are heuristically modified to add the essential differences between DLA and its continuum limit: the presence of noise and the existence of a microscopic cutoff. This leads to a new model which is hoped to be in the same universality class as DLA. Even if it is not in the same universality class, it is similar enough to be of interest in itself.

Second, under an adiabatic assumption, the equation is modified to vastly simplify the time dependence, leaving almost a static problem. The adiabatic assumption

makes possible the RG and perturbation theory calculations described latter in the thesis. The adiabatic assumption is justified by numerics and self-consistently by the RG itself.

At this point, before doing the RG, it is still possible to make some comparison to numerics based on the continuum representation of DLA.

Third, a perturbation theory is developed for the continuum equation, with a well defined set of rules for calculating correlation functions. The perturbation theory requires some resummation of diagrams, where to calculate resummed propagators it is necessary to use a renormalization group approach. This RG forms the fourth part of the thesis; the calculations for the RG have only been done to lowest order, producing an appropriate renormalized propagator and vertex. Fifth, the adiabatic assumption is removed, and the renormalized propagator is used to calculate various exponents in the theory. Sixth, the results are compared to numerical experiments, the self-consistency of the approach is discussed, and there is discussion of what may happen if the computation is performed to higher orders.

Unfortunately, there are some disadvantages to the techniques used in this thesis. After performing the RG, a small dimensionless parameter appears, equal to $1/5$. Expansion is carried out order by order in this parameter. This suggests that the theory presented below is close to some trivial fixed point at which the coupling would vanish; it is possible that the trivial fixed point may be found by varying a parameter α to be defined below. Since the RG has not as yet been carried out for all values of α, the existence of the trivial fixed point is not yet verified, and thus the nature of the perturbation expansion is somewhat unclear.

In addition, the perturbation expansion that will be used, although looking very similar to those used in field theory, cannot be derived from a functional integral in any simple fashion. This means that there may exist some doubt about the validity of field theory techniques in this problem, and certain questions about the renormalization of quantities such as noise and interaction.

On the other hand, the major advantage of the theory is that, by dealing directly with an analytic function describing the envelope of the cluster, it provides a very

natural means of defining different scales in the problem, and of coarse-graining a cluster while only slightly modifying the solution of Laplace's equation outside the cluster.

1.7 Notation

A large number of functions will need to be defined in this thesis. As much as possible, I will use the following notations. Capital letters are used for functions, such as F, G to be defined latter, which describe the shape of a specific growing aggregate. Power series expansions of these functions will be denoted by subscripts, so $F(z) = F_1 z^1 + F_0 z^0 + F_{-1} z^{-1} + ...$ In the continuum limit of these power series expansions, to be appropriately defined latter, where sums are approximated by integrals, the Latin letters j, k, l, m, n, o will be used as indices. One will see terms like $G(j)$.

Greek letters ϵ, Λ, μ will be used for ultraviolet and infrared cutoffs in these continuum laws.

Greek letters α, λ_0 will be used for various parameters in the models defined in this thesis.

Lower case letters will be used for functions which define growth rules for the aggregate. These include the functions f, s, t defined latter.

Latin letters x, z represent points in the complex plane. The number t represents time, either as a discrete number of steps or as a real number in a continuum limit. The numbers θ, ϕ represent angles, while the function $\theta(j)$ is the step function.

Unless otherwise specified, subscripts attached to functions will be used to denote derivatives, thus F_x is the derivative of F with respect to x. As an exception to this, the expression $f_{\lambda,\theta}(z)$ will represent a function parametrized by λ and θ.

Chapter 2

Conformal Model and Continuum Growth Law

A model for growth is defined. From this model, the Shraiman-Bensimon equation is derived for a function F which maps the unit circle in the complex plane onto the boundary of the growing object. Defining

$$G = \frac{1}{F_z} \tag{2.1}$$

and making some approximations, we obtain a continuum growth rule, equation (2.32), which still includes effects of noise and finite cutoff.

2.1 Conformal Model

The following model for DLA in terms of conformal mappings leads to results that are apparently numerically equivalent to DLA[20]. It should be noted that the RG in this thesis relies upon a continuum approximation to this model; this continuum approximation could also have been obtained from the lattice version of DLA without reference to the conformal mapping model, but the conformal mapping model provides a better justification for the continuum equation.

In this method, we deal only with the analytic function F, which is defined as the

analytic function which maps the unit circle in the complex plane onto the boundary of the growing cluster. We introduce two parameters, α and λ_0, where $\alpha = 2$ corresponds to DLA and λ_0 is some constant determining the size of an individual random walker. To grow the object, first pick a random point $x = e^{i\theta}$ on the unit circle. Then, calculate $F_z(x)$, which is the derivative of F at this point. We define

$$\lambda = \lambda_0 (F_z(x) F_z^*(x))^{-\alpha/2} \tag{2.2}$$

The case of $\alpha = 2$ will correspond to DLA and it is that case that will be considered from now on; other cases will be briefly discussed in the conclusion. Then in a given growth step, $F(z)$ is replaced by

$$F(f_{\lambda,\theta}(z)) \tag{2.3}$$

where f is a function that produces a small bump at angle θ, with linear dimension of the bump of the order of the square root of λ. λ, θ are parameters that define the function f. An explicit example of $f_{\lambda,0}$ is given by:

$$\left[\frac{1+\lambda}{2z}(z+1) \left(z + 1 + \sqrt{z^2 + 1 - 2z\frac{1-\lambda}{1+\lambda}} \right) - 1 \right]^{1/2} z^{1/2} \tag{2.4}$$

For $\theta \neq 0$, we have $f_{\lambda,\theta}(z) = e^{i\theta} f_{\lambda,0}(e^{-i\theta} z)$.

In the small λ case, f reduces to

$$z + \lambda z (z + e^{i\theta})/(z - e^{i\theta}) \tag{2.5}$$

and by averaging over angle we may determine a continuum growth law. A picture of a cluster produced by this growth rule is shown in Fig. 1. A picture of the effect of the mapping f on the unit circle is shown in Fig. 2.

The numerical implementation of the conformal model is discussed in Appendix B.

2.2 Why the Conformal Mapping Model Works, Why $\alpha = 2$

As is well known, DLA as conventionally defined in terms of random walkers has various conformal properties, resulting from the possibility of expressing the probability of a walker arriving at a given point on the surface in terms of a local electric field. Due to conformal invariance of Laplace's equation, one can calculate the local electric field at a given point on the surface of the object by finding a function $F(z)$ which maps the unit circle to the surface of the object. Then, one can take a field $\phi(z)$ to be equal to $\mathrm{Re}(ln(z))$ outside the unit circle and $\mathrm{Re}(ln(F^{-1}(z)))$ outside the growing cluster. From this one can calculate the field strength outside the cluster. One finds that the field strength is proportional to $1/|F'(z)|$. This implies that the measure $E\,ds$ on the surface of the cluster transforms to $d\theta$ on the surface of the circle, when one takes into account the Jacobians relating arc length $d\theta$ on the circle to length ds on the cluster.

Therefore, the probability to add a walker to a given point on the boundary of the circle is constant over the whole circle. This is why we pick random angles θ in the previous section. One may see that, by composing functions $F(f(z))$ as done in the previous section, one produces an additional bump on the contour of the cluster at the appropriate point. The only task is to tune the size of the bump in f to produce a bump of constant size. By considering the local Jacobian, one realizes that the area of the bump in f must be proportional to $1/|F'(e^{i\theta})|^2$. This area is parameterized by λ, and so this justifies the above rule for picking λ.

One may consider values of α different from 2. The continuum equation of motion for the conformal model at given α is equal to the continuum equation of motion for the dielectric breakdown model[3] at $\eta = \alpha - 1$. However, the actual dynamics are different, since in the dielectric breakdown model one has a constant bump size, with probability of adding a bump at a given point dependent on η, while in the conformal model one has a probability of adding a bump independent of α, with a bump size dependent on α. A numerical study[20] found a phase transition in the

conformal model at $\alpha = 1$ from stable to unstable growth. The exact relation between the conformal model and the dielectric breakdown model is still unclear. Appendix C contains a discussion of numerical results at varying values of α. Some of the inspiration for the renormalization group approach derives from the renormalization of λ_0 at values of $\alpha < 1$.

2.3 Continuum Growth Law

The continuum growth law for DLA is known to be equivalent to the Hele-Shaw dynamics, which obeys the law

$$\mathrm{Im}(F_t F_\phi^*) = 1 \tag{2.6}$$

where F is a function which maps the unit circle in the complex plane onto the boundary of the aggregate and subscripts denote derivates with respect to time or to angle ϕ on the circle. This law may be rewritten as

$$\begin{aligned} \mathrm{Re}(F_t/zF_z) &= 1/(F_z F_z^*) \\ \mathrm{Re}(F_t \tfrac{|F_z|}{zF_z}) &= 1/|F_z| \end{aligned} \tag{2.7}$$

where here $z = e^{i\phi}$. Finally, this second growth law may be rewritten as

$$F_t = F_z \int \frac{d\theta}{2\pi} \Big(F_z(e^{i\theta}) F_z^*(e^{i\theta}) \Big)^{-1} z \frac{z + e^{i\theta}}{z - e^{i\theta}} \tag{2.8}$$

This equation, the Shraiman-Bensimon equation, results from substituting the small λ expansion of equation (2.5) into the equation (2.3) for the dynamics of F, where $F(f(z))$ is approximated by $F(z) + F_z(z)(f(z) - z)$.

In the Shraiman-Bensimon equation, one may divide both sides by zF_z and then take the real part of both sides. This will recover equation (2.7) and show that the two equations are equivalent. Equation (2.7) implies that the normal velocity of the surface at a given point is proportional to the local electric field at that point.

Equation (2.5) may be rewritten as (taking $\theta = 0$ for simplicity)

$$z + \lambda z(z+1)/(z-1) = z + \lambda z(1 + 2/z + 2/z^2 + 2/z^3 ...) \tag{2.9}$$

Therefore, the effect of the integration over angle in the continuum growth law is to project out negative Fourier components in λ considered as a function of angle. The factor of 2 difference between the zeroth component and all other components will be important later.

It will also be useful to define a continuum law for another function G which is defined by equation (2.1). This function has several advantages. The equation for λ then becomes

$$\lambda = \lambda_0 G(x) G^*(x) \tag{2.10}$$

which has a simpler form than equation (2.2). This has a physical interpretation that G determines the strength of the electric field at point x. Also, G is the derivative of the inverse function of F and the inverse function of F has a more natural growth rule than F does. That is, if $F^{-1}(F(z)) = z$, then under a growth step with given λ and x, the function $F^{-1}(z)$ changes into $f^{-1}(F^{-1}(z))$. The continuum law for G, as obtained by using the definition of G and the growth law for F, is

$$\begin{aligned} G_t &= G_z \int \tfrac{d\theta}{2\pi} G(e^{i\theta}) G^*(e^{i\theta}) z(z + e^{i\theta})/(z - e^{i\theta}) \\ &\quad -G \int \tfrac{d\theta}{2\pi} G(e^{i\theta}) G^*(ei\theta) [z(z + e^{i\theta})/(z - e^{i\theta}]_z \end{aligned} \tag{2.11}$$

It is also useful to consider the continuum growth laws for the power series of F and $G(z)$. Writing

$$F(z) = F_1 z^1 + F_0 z^0 + F_{-1} z^{-1} + ... \tag{2.12}$$

$$G(z) = G_0 z^0 + G_{-1} z^{-1} + G_{-2} z^{-2} + ... \tag{2.13}$$

then equation (2.11) is equivalent to

$$(G_{-j})_t = (j - 2k - 1) \sum_{k,l,m} G_{-k} G_{-l} G^*_{-m} \delta(k + l - m - j) 2\theta(j - k) \tag{2.14}$$

where the discrete step function is defined by

$$\theta(j-k) = \begin{cases} 1 & \text{for } j > k \\ 1/2 & \text{for } j = k \\ 0 & \text{for } j < k \end{cases} \tag{2.15}$$

An continuum equation may also be written for the power series expansion of F, but we will not need to use such an equation.

There are some problems with directly applying the continuum growth law above, in any of its forms, to the discrete random process that defines DLA. The continuum law leads to the appearance of cusps in the contour of the cluster after a finite time, and the continuum law is deterministic while the discrete law is random. However, the continuum law must have some applicability to the discrete cluster growth, because, for example, the conserved quantities of the continuum law are approximately conserved by the random process[21]. Thus, we will try, in the rest of this chapter, to correct the problems in the continuum law so that it may be of some use in describing the discrete, random growth process.

2.4 Ultraviolet Cutoff

The above formulation of the problem suggests a method, outlined in this section, of inserting an ultraviolet cutoff into the growth law. This cutoff will be inserted by hand, and then the parameter of the cutoff will be adjusted to obtain the correct microscopic scale.

In the discrete conformal mapping model, F never develops cusps because f is always well behaved. The specific form of f does not matter; all that matters is that the approximate expansion for f given by $f(x) = z + \lambda z(1 + 2/z + 2/z^2 + ...)$ is only correct for small negative powers of z. The power series expansion of f is cutoff at some point because f is well behaved. This cutoff depends on λ, which itself depends on the angle θ at which growth is taking place. The approximation made in inserting the ultraviolet cutoff into the continuum law is that *the cutoff in the power series*

expansion for f depends only the average value of λ over the circle at the time of a given growth step, and not on the exact value of λ where the growth is occurring, where the dependence on the average value of λ is chosen in such a way as to produce the correct microscopic scale in the DLA growth process.

Then a simplification follows. Suppose the regularized form of f is chosen to be

$$f(z)_{\lambda,\theta} = z + z\lambda\frac{(1+\epsilon)z + e^{i\theta}}{(1+\epsilon)z - e^{i\theta}} \tag{2.16}$$

where ϵ is a fixed function of $\langle\lambda\rangle$, which is defined to be the average value of λ over the entire circle.

It is worthwhile also to define

$$\Lambda = 1/\epsilon \tag{2.17}$$

Then Λ represents the highest power of z that will occur in the growth law.

Let us make a change of variable. We will replace $F(z)$ by the function $F((1+\epsilon)^{-1}z)$ and $G(z)$ by $G((1+\epsilon)^{-1}z)$. At the same time f is replaced by $(1+\epsilon)f((1+\epsilon)^{-1}z)$. Then the continuum law (2.8) for F becomes

$$F_t = F_z \int \frac{d\theta}{2\pi}\Big(F_z((1+\epsilon)e^{i\theta})F_z^*((1+\epsilon)e^{i\theta})\Big)^{-1} z\frac{z+e^{i\theta}}{z-e^{i\theta}} \tag{2.18}$$

where now the cutoff dependence has been moved to the derivatives of F. The continuum law (2.11) for G becomes

$$\begin{aligned} G_t &= G_z \textstyle\int \frac{d\theta}{2\pi} G((1+\epsilon)e^{i\theta})G^*((1+\epsilon)e^{i\theta})z(z+e^{i\theta})/(z-e^{i\theta}) \\ &\quad -G \textstyle\int \frac{d\theta}{2\pi} G((1+\epsilon)e^{i\theta})G^*((1+\epsilon)e^{i\theta})[z(z+e^{i\theta})/(z-e^{i\theta}]_z \end{aligned} \tag{2.19}$$

The value of ϵ must now be calculated.

Before the averaging process, the dependence of the cutoff on λ is easy to determine by, for example, expanding the function f as defined by equation (2.4). After the averaging process, it is not necessarily the case that the average cutoff ϵ will be determined in the same way from the average value of λ. The averaging may introduce nontrivial behavior. Instead I will look for the dependence of ϵ on the cluster size;

since the cluster size and the average of λ are related, this is an equivalent procedure.

Expanding the cutoff in the continuum growth law to linear order in ϵ yields an additional term in the equation for F_t. This additional term changes equation (2.7) to

$$\mathrm{Re}\Big(F_t \frac{|F_z|}{zF_z}\Big) = 1/|F_z| - 2\epsilon \mathrm{Re}\Big(\frac{zF_{zz}}{F_z|F_z|}\Big) \tag{2.20}$$

The additional term may be written as

$$2\epsilon\, \mathrm{Im}\left(\frac{F_{\phi\phi}}{F_\phi|F_\phi|}\right) = 2\epsilon/R \tag{2.21}$$

where $z = e^{i\phi}$ and R is the local radius of curvature. This is a surface tension term.

The basic idea will be to adjust ϵ to produce the correct size for microscopic features; this size is the size of an individual walker in the lattice formulation of DLA.

A dimensional analysis argument may help understand the size of the cutoff. This dimensional analysis argument will relate the dependence of cutoff on macroscale to the dependence of cutoff on microscale.

The function $F(z)$ may be assigned the dimension of length, and z may be made dimensionless. This means that we are interpreting z as a parametrization of the cluster. Then both Λ and ϵ are dimensionless. We know that Λ must be a function of the size of an individual walker, but then since the dimensional argument implies that Λ is dimensionless, Λ must be proportional to some power of the ratio of the size of the object to the size of an individual walker, as this is the only way to form a dimensionless number. Let r_0 denote the length scale of an individual walker.

Let us see how to measure the linear size of the object. Recalling the expansion of F in Fourier coefficients given by equation (2.12), by a theorem on univalent functions [23] the size of the object is at most 4 times F_1, the leading term of the power series. Asymptotically, F_1 will measure the size of the object.

To fix the minimum radius of curvature at r_0, the size of an individual walker, the cutoff ϵ must be chosen so that ϵ/R, the surface tension term, balances the electric field at the given radius. To determine the radius at which they balance, we need

to make an assumption about the singularities of G. Let us assume G has simple poles and therefore F_z has simple zeroes. Suppose we look at points near a zero of F_z. Without loss of generality, take this zero to be at point z_0 where $z_0 = 1 - \delta$ with δ some small positive number. Locally we find

$$F_z \propto z - z_0 \tag{2.22}$$

The electric field at $z = 1$ is proportional to $1/\delta$. The radius of curvature at $z = 1$ is proportional to $1/\delta^2$. For the surface tension to balance the electric field we require

$$1/\delta = \epsilon/\delta^2 \tag{2.23}$$

This implies that $\delta = \epsilon$. Then, since $R = 1/\delta^2$, we need that $\epsilon = \sqrt{R}$. If R is equal to r_0, we find

$$\epsilon \propto r_0^{1/2} \tag{2.24}$$

The dimensional argument then implies that $\epsilon \propto (r_0/F_1)^{1/2}$, where now the proportionality constant is dimensionless. This implies that

$$\Lambda \propto (F_1/r_0)^{1/2} \tag{2.25}$$

In the actual growth, F_1 is changing in time, but r_0 is constant. Thus the time dependence of Λ is determined by $\Lambda \propto F_1^{1/2}$. As expected, the cutoff is increasing in time. If the power series expansion for G is defined by equation (2.13), then

$$G_0 = 1/F_1 \tag{2.26}$$

so that it is also possible to measure the size of the object using the power series expansion of G.

As a further explanation of the dimensional analysis argument, it may be directly shown that, if the cluster is approximately circular, with a small bump on it, then the dependence of Λ on the cluster size is correctly given by equation (2.25). The

approximate circularity means that instead of simply stating that the electric field is proportional to $1/\delta$ and that the radius of curvature is proportional to $1/\delta^2$, we keep track of the proportionality constants in terms of F_1, and then directly show that $\epsilon \propto (r_0/F_1)^{1/2}$. The advantage of the dimensional argument is that it is possible to make this argument without any assumptions on the macroscale of the cluster; the dependence of Λ on r_0 follows from microscopic considerations, and the dimensional analysis argument then yields the dependence on F_1.

One might worry that for the actual aggregate the poles will not necessarily be simple poles. As Halsey et. al. have shown [24], the surface is described by wedges with a non-zero opening angle, and the singularities exist on a fractal set. However, the continuum growth law of equation (2.11) only produces simple poles in G. It is only the dynamics that lead apparently to the creation of non-simple poles, via an accumulation of simple poles. Therefore, the cutoff will be imposed as if the poles were simple.

Because the object grows, Λ increases with time. This is what leads to nontrivial dynamics and to a fractal dimension less than 2. If instead of varying with time, the cutoff Λ were held constant, then the aggregate would asymptotically grow at a Λ-dependent rate proportional to the square root of time, and would have a fractal dimension of 2.

2.5 Noise

From now on, G will be the function of interest and F will be ignored. There are two reasons for this: the continuum law for G is simpler, and noise may be more easily inserted into the law for G. The actual growth of G is not deterministic; we may write the actual growth of G symbolically as follows: actual growth of G = continuum growth of G + (actual growth of G − continuum growth of G). The term in parenthesis represents noise. This noise term will be written as

$$sG^f(z) \tag{2.27}$$

where s is a constant with dimensions of inverse time and G^f is some function of z. We approximate that G^f vanishes on average. If we expand G^f in a series as $G^f_{-1}z^{-1} + G^f_{-2}z^{-2} + ...$, we will write the average of $G^f_i G^{f*}_j$ as

$$\langle G^f_i G^{f*}_j \rangle = \delta_{ij} N(j) \tag{2.28}$$

where N is some unspecified function. We will also assume that any average of several G^f can be written as a product of pairwise averages. These are the essential approximations in the noise.

With noise included, we modify equation (2.19) to

$$\begin{aligned} G_t &= G_z \int \tfrac{d\theta}{2\pi} G((1+\epsilon)e^{i\theta}) G^*((1+\epsilon)e^{i\theta}) z(z+e^{i\theta})/(z-e^{i\theta}) \\ &\quad -G \int \tfrac{d\theta}{2\pi} G((1+\epsilon)e^{i\theta}) G^*((1+\epsilon)e^{i\theta}) [z(z+e^{i\theta})/(z-e^{i\theta}]_z + sG^f(z) \end{aligned} \tag{2.29}$$

The notation G^f is used for the noise because, in the perturbation theory, the function G^f will play a role similar to a *free* field in field theory.

The approximations are justified for two reasons. Since the noise is essentially generated by the dynamics, that is a small amount of noise will be amplified by the continuum growth, the dynamics should not be very sensitive to how the noise is inserted. This means we need not worry about the exact form of $N(j)$. Second, since the actual growth law for F^{-1} is rather simple, involving a function acting on F^{-1}, it is most natural to insert the noise into F^{-1}, or into G, which is the derivative of F^{-1}. Inserting the noise into the growth law for F, which has a more complicated growth law, may have a different effect on the overall dynamics.

2.6 Continuum Limit In Momentum Space

In order to make the RG calculations easier, I will also take a continuum limit for the Fourier components of G and G^f. This will result in replacing the discrete sums of equation (2.14) with integrals. This amounts to a change in the geometry of the growth; instead of parametrizing the boundary of the growing cluster by a point on

the unit circle, we will parametrize it by a point on the real line in the complex plane.

In the neighborhood of a given point on the unit circle, such as $z = 1$, the unit circle is locally approximated by a straight line. As we look at shorter and shorter length scales, this approximation becomes more and more accurate. The equation $z = e^{i\theta}$ is approximated by $z = 1 + i\theta$. Thus, on short scales, in the neighborhood of $z = 1$ we can approximate

$$F(z) = F_1 z^1 + F_0 z^0 + F_{-1} z^{-1} + ... \approx F_1(1 + i\theta) + F_0 + \int dj\, F(j) e^{-ij\theta} \tag{2.30}$$

$$G(z) = G_0 z^0 + G_{-1} z^{-1} + G_{-2} z^{-2} + ... \approx G_0 + \int dj\, G(j) e^{-ij\theta} \tag{2.31}$$

where $F(j)$ and $G(j)$ should be considered as being defined by the above equations. They are defined so that j is always a positive quantity. This approximate form for $G(z)$ will break down for θ of the order of 1 radian. This implies that the Fourier expansions will break down for low values of j. This has the effect of an infrared cutoff; the cutoff will be at j of order μ, which is a number of order 1. The cutoff μ is constant in time, unlike Λ, but under the RG we will find it convenient to rescale μ. After introducing the equation of motion appropriate to this approximate expression for G, I will then explain the effect of nonzero μ on this equation.

The symbol j in equations (2.30),(2.31) will be referred to as a momentum since it will play a role in the perturbation theory of the next chapter equivalent to that of a momentum in a perturbation theory for a field theory.

We take equation (2.14) and transcribe it to this continuum approximation. Noise is added as in equation (2.29). The result is:

$$\begin{aligned} G_t(j) \;=\; & (1/\mu) \textstyle\int dk\, t(j,k)\, G(k) \int\int dl\, dm\, G(l) G^*(m) \exp(-(l+m)/\Lambda) \\ & \times \delta(k + l - m - j) 2\theta(j - k) + s G^f(j) \end{aligned} \tag{2.32}$$

where $t(j,k)$ is some general function (initially it is proportional to $(j - 2k - 1)$ as in equation 2.14), and where the factor of $1/\mu$ is inserted to produce the correct dimensions for t in the RG, as will be clear later. The insertion of the factor of $1/\mu$ simply

amounts to a redefinition of $t(j,k)$. The function t will flow under the renormalization group. The exponential term is the appropriate version of the ultraviolet cutoff in the continuum limit. We define the continuous step function θ by the same equation (2.15).

The effect of the cutoff μ is twofold: the δ-function in equation (2.32) has a nonzero width of order μ, and hence a finite height. The quantity $\delta(0)$ is of order $1/\mu$. Also in the definition of the noise, equation (2.28) is replaced by:

$$\langle G^f(i) G^{f*}(j) \rangle = \delta(i-j) N(j) \tag{2.33}$$

where again the δ-function has a nonzero width.

By rescaling momentum, the cutoffs μ and Λ may be changed, but the ratio of the two cutoffs will remain constant. The purpose of the RG will be to integrate the upper cutoff from Λ to $\Lambda - \delta\Lambda$. Then, for the sake of convenience, the upper cutoff will be rescaled back to Λ. The assumption is made that when Λ is much greater than μ this renormalization does not change the essential physics of the system.

Physically, equation (2.32) describes the problem of DLA growth in the upper half of the complex plane, where the boundary of the growth is parametrized by a point θ on the real axis. The cutoff μ has the physical interpretation that growth only occurs in a finite width on this axis.

For use later, let us define a functional $\widehat{W}$ such that

$$\begin{aligned} \widehat{W}[j, G(k), G(l), G^*(m)] &= (1/\mu) \int dk\, t(j,k)\, G(k) \int\int dl\, dm\, G(l) G^*(m) \exp(-(l+m)/\Lambda) \\ &\quad \times \delta(k+l-m-j) \end{aligned} \tag{2.34}$$

Thus, the right hand side of equation (2.32) is $\widehat{W}[j, G(k), G(l), G^*(m)] + sG^f(j)$. The functional $\widehat{W}$ is linear in each of its last three arguments.

Chapter 3

Adiabatic Assumption and Numerical Predictions

3.1 Adiabatic Assumption

An important approximation is made, which changes the problem to one of describing an aggregate which is statistically unchanging in time. In the end, we will describe aggregates whose average size and roughness remain constant.

The cutoff Λ is slowly changing in time. As the object grows, Λ changes more and more slowly. The exact structure of the cluster at a given time depends upon its growth at all previous times, but since the object spends a long time growing with an approximately fixed cutoff, it is expected that the structure of the object at a given time t with resulting cutoff Λ is determined only by its growth during previous times t' with resulting cutoffs Λ' such that Λ' is very close to Λ. Times t' such that Λ' is very different from Λ will be so far in the past that we do not expect them to alter the structure of the cluster.

Furthermore, if the cutoff is fixed, the equations of motion are homogeneous, in the sense that up to a rescaling of time and noise, two clusters, which differ only by a change of scale, will have exactly the same growth for the same random noise. More precisely, if $G(t)$ is a solution of the equation (2.29), with fixed cutoff Λ and given noise G^f, then, for any number b, the function $bG(b^2t)$ is a solution of equation (2.29)

with the same cutoff Λ and with noise bG^f and s replaced by $b^2 s$.

For a large object it is then reasonable to make the adiabatic assumption that, despite the changing cutoff, *up to a rescaling of the cluster, the statistical properties of the function G at some given time with some given cutoff Λ are well described by evolving an arbitrary initial G for sufficiently long time using the equations of motion with the cutoff held fixed at that value Λ.*

First, we will analyze the dynamics of G in the fixed cutoff problem, and then we will use the adiabatic assumption to relate it to the changing cutoff problem.

Let us take equation (2.32) and, holding the cutoff fixed, make a dynamical rescaling of the function G as it evolves under this equation. After every time step of length dt we will rescale G to $(1 - s\,dt)G$. Then, the rescaled G satisfies the equation of motion

$$\begin{aligned} sG(j) + G_t(j) &= (1/\mu) \int dk\, t(j,k) G(k) \int\int dl\, dm\, G(l) G^*(m) \exp(-(l+m)/\Lambda) \\ &\quad \times \delta(k + l - m - j) 2\theta(j - k) + sG^f(j) \end{aligned} \tag{3.1}$$

On average, the rescaled G has constant size.

The amount by which the cluster is rescaled per unit time, s, is the same s referred to in the section on Noise. It is simply a matter of notational convenience to chose these two numbers s to be the same. Any other choice of s in the section on noise simply amounts to a redefinition of G^f.

The function G before rescaling is growing in time. To determine how rapidly an unrescaled cluster of given size and given, fixed cutoff grows, we may follow this procedure: evolve a rescaled cluster using equation (3.1) with an s chosen such that the rescaled cluster is of the desired size. Then, from the value of s needed to maintain the desired size, determine the growth rate of the unrescaled cluster. For the unrescaled cluster, the average of $\frac{d \log(G_0(t))}{dt}$ is equal to s.

Under the adiabatic assumption, we can now take the growth rate for the fixed cutoff problem, this growth rate being a function of the size of the cluster and the cutoff, and use it to determine the growth rate for a cluster with a changing cutoff. To determine the growth rate of a cluster of given size in the changing cutoff problem

one can determine the cutoff from the size of the cluster, using equation (2.25), and then calculate the growth rate of a cluster of the same size in the fixed cutoff problem, using the rescaling trick to determine how quickly that cluster grows.

Under RG scaling, in fact, we will find that the equation of motion changes in such a way that s changes; in fact, s may acquire momentum dependence. Before RG scaling s will be negative, since F is increasing, causing G to decrease. After RG flow, an appropriate combination of t, s, and G^f goes to a universal value. The adiabatic assumption will mean that we assume that at every instant in the original DLA problem, the function G is described by a function in the long time limit of the problem with a fixed cutoff and a rescaling term s, where s is picked to obtain the correct overall scale for G.

On average, G_t in equation (3.1) vanishes. What is left of G_t after the rescaling process is just fluctuations about the average growth. There may in fact be solutions such that G_t vanishes identically, but this is unimportant. In the RG, even with G_t non-zero, the s term and interaction term (G^3 term) will determine the nature of the aggregate. As will be shown, under RG flow, the G_t term flows under RG so that, the fluctuations in $G_t(j)$ decrease as j decreases. The lower momentum terms then, in the unrescaled problem, will have their growth more accurately given just by the sG term. Fluctuations about this overall growth will be less.

3.2 Numerical Predictions

It will be worthwhile to mention at this point that already some definite numerical predictions can be extracted from the above work. Since the RG that follows relies upon the continuum equations, it is good to independently check the validity of these equations for describing DLA.

If any RG is to hold, the coefficients of G must obey some scaling law. In the last chapter of this thesis, such a scaling law will be shown numerically. The coefficients decay with a power law. It will be the purpose of the RG to calculate this power law.

Since the absolute value of G is equal to the local electric field, there is a close

connection between G and the multifractal exponents of references [10, 11, 12]. These exponents are defined by equations (6.7),(6.11). The $(2n+1)$-th power of the electric field, integrated over the object, is given by $\int d\theta (G(\theta)G^*(\theta))^n$. This integral over θ can be converted to an integral over components of G in momentum space. Cutting those off at momenta Λ is equivalent to cutting the real space integration off at a length scale of order Λ^{-2}. Since the multifractal exponents are defined in terms of the scaling of powers of the electric field against length, we obtain an equivalent definition of multifractal exponents in terms of scaling of powers of G against cutoff. This discussion of exponents will be done in more detail later, after the RG permits us to calculate these exponents analytically.

As a check of the adiabatic assumption, a numerical simulation was performed using the original discrete conformal mapping model defined in chapter 1, section 2. In this simulation, after every growth step, the object was shrunk by some constant factor. Visually we could not see any difference, in the growing region on the surface, between the cluster shrunk after every growth step and another cluster which was not shrunk. A calculation of fractal dimension also failed to show any significant differences.

Chapter 4

Perturbation Theory

A perturbation theory is developed for the equation of motion (3.1). This permits in principle the calculation of any correlation function of the theory in terms of noise averages. In practice, a resummation of the series is employed which expresses multi-point correlation functions in terms of two-point correlation functions.

4.1 Perturbation Rules

Using the adiabatic assumption, the equation of motion (3.1) looks very much like the variation of an action. Although there no such action can be found, a perturbation theory will be developed, based on this analogy, to permit the use of techniques from field theory.

This technique is very similar to that used, for example, in solving the Navier-Stokes equation [25, 26]. Such a perturbation theory has been known for many years. Before proceeding with the details, let me summarize the essential attributes: a perturbation theory is developed by expanding G in powers of the noise, G^f, and expanding correlation functions of G in terms of two-point correlation functions of the noise. Since the noise is amplified by the dynamics of equation (3.1), this expansion is not expected to converge. However, after resummation of the series, it becomes possible to replace this by an expansion not in the two-point correlation function of the noise, but in the two point correlation function of G itself. Further, a resummation of series

leads to a resummed propagator (defined below). Unlike the Navier-Stokes perturbation theory for turbulence[25, 26], it will not not be necessary to define a resummed interaction vertex. The above procedure leads to a well defined perturbation series in "skeleton" diagrams. One point that will be necessary in the following treatment that is not necessary in the case of turbulence is that G is a complex field, and thus the propagators will be directed lines; the notation that follows will therefore differ from that seen in Navier-Stokes problems.

The perturbation theory is constructed as follows: the equation of motion (3.1) permits us to solve for $G(j)$ in terms of a cubic in $G(j)$. Using the definition of $\widehat{W}$ in equation (2.34) we write

$$G(j) = \left(s(j) + \frac{\partial}{\partial t}\right)^{-1} \left(\widehat{W}[j, G(k), G(l), G^*(m)] + s(j)G^f(j))\right) \tag{4.1}$$

where $s(j)$ is used instead of s because s may, under RG flow, acquire j dependence.

The operator $(s(j) + \frac{\partial}{\partial t})^{-1}$ may be expanded as a formal power series in $\frac{\partial}{\partial t}$. In Navier-Stokes perturbation theory, this operator is referred to as the propagator, in analogy with a similar object in field theory.

We may then iteratively solve equation (4.1) as follows

$$\begin{aligned} G(j) &= \tfrac{1}{s(j)}\widehat{W}[j, G(k), G(l), G^*(m)] + G^f(j) + \mathrm{O}(\tfrac{\partial}{\partial t}) \\ &= \tfrac{1}{s(j)}\widehat{W}[j, G^f(k), G^f(l), G^{f*}(m)] + G^f(j) \\ &\quad + \tfrac{1}{s(j)}\widehat{W}[j, \tfrac{1}{s(k)}\widehat{W}[k, G(n), G(o), G^*(p)], G^f(l), G^{f*}(m)] \\ &\quad + \ldots \\ &\quad + \mathrm{O}(\tfrac{\partial}{\partial t}) \\ &= \ldots \end{aligned} \tag{4.2}$$

The iterative solution of equation (4.1), by solving for the values of $G(k)$, $G(l)$, and $G^*(m)$ on the right hand side, is an expansion in powers of the interaction, t. This is simultaneously an expansion in powers of the noise, G^f. The zeroth order and first order terms in t, and one of the second order terms, have been written in equation (4.2). At any point in the process, one can stop the perturbation expansion by setting

$G(j) = G^f(j)$ plus higher orders in $\frac{\partial}{\partial t}$. Thus, in the perturbation expansion for G one sums at every stage over two possible expressions for G:

$$\begin{aligned} G(j) &= (1/s(j))(1/\mu) \int dk\, t(j,k) G(k) \int\int dl\, dm\, G(l) G^*(m) \exp(-(l+m)/\Lambda) \\ &\quad \times \delta(k+l-m-j) 2\theta(j-k) + \mathrm{O}(\tfrac{\partial}{\partial t}) \end{aligned} \tag{4.3}$$

or

$$G(j) = G^f(j) + \mathrm{O}(\frac{\partial}{\partial t}) \tag{4.4}$$

These operations can be represented graphically with Feynman diagrams, in which t is an interaction term and s is like a mass term. This leads to a series of diagrams for G. These diagrams have no loops.

The quantities computed as described above depend upon the specific realization of the noise. Since we are interested in average quantities, we will compute correlation functions. A correlation function is defined as an average over noise of a product of several $G(j), G^*(j)$ with the same total number of G and G^*, and will be written as

$$\langle G(j_1) G(j_2) ... G(j_n) G^*(k_1) G^*(k_2) ... G^*(k_n) \rangle \tag{4.5}$$

When computing these averages, the average over noise must be taken. This is done by taking noise terms resulting from the above expansion for G and G^* and contracting them with each other in all possible pairwise fashions. Each contraction of two noise terms at momenta j, k leads to a factor of $\delta(j-k)N(j)$, as given by equation (2.33). This leads to diagrams with loops.

Fig. 3 indicates how diagrams for the theory are drawn. There are three types of diagrams that may be drawn. They are drawn in essentially the same fashion, except that different meanings are assigned to the external lines and different numbers of noise contractions are included. A diagram for a correlation function has one external line for each term in the correlation function to be computed. Diagrams for quantities other than correlation functions may have different meanings assigned to the external lines. These diagrams all involve one or more external lines being expressed as a

function of the other external lines. This may occur either as an expansion of G directly in terms of the noise, or as a piece of a diagram that occurs inside another diagram. For example, the diagram (a) in Fig. 3 is not itself a correlation function, but it represents a term that may occur inside a computation of a correlation function. For this diagram, the line for $G(j)$ is expressed in terms of other lines, which in turn may be set equal to the noise, or may be further expanded.

The notation for diagrams is the following: crosses denote contractions on noise, and the directions of the lines indicate complex conjugation and orientation within the diagram. A line may be said to carry momentum j; when two lines are contracted, they must carry the same momentum and all external lines are assigned a momentum determined by the particular correlation function to be computed. A t vertex has 2 lines entering and 2 lines leaving, corresponding to G and G^*. The $G(j)$ line for a $t(j,k)$ vertex is drawn as entering, the $G^*(m)$ is drawn as entering since it is complex conjugated, while the other lines are drawn as leaving the vertex. The j and k lines will always be drawn parallel to each other in a t vertex; the l and m lines will be drawn at an angle. The distinction must be made between j,k and l,m because j and k enter into t while l and m are summed over blindly.

The rules for diagrams for correlation functions may be summarized as follows: to calculate the average of the product of $G(j_1)G(j_2)...G(j_n)G^*(k_1)G^*(k_2)...G^*(k_n)$, where j_i, k_i are various numbers: draw one external line for each term in the correlation function. The terms in G should be drawn as entering the diagram with momentum j_i, while those for G^* should be drawn as leaving the diagram with momentum k_i. Draw all possible diagrams, assigning a factor of $t(j,k)2\theta(j-k)$ to each vertex and a factor of $1/s(j)+\mathrm{O}(\frac{\partial}{\partial t})$ for each line, while conserving the sum of ingoing and outgoing momentum at each vertex. For each noise contraction assign a factor of $s^2(j)N(j)$. Finally, the perturbation theory may give rise to a term such as $\theta(0)$. This will arise from something like $\int dj\delta(j-k)\theta(j-k)$. While $\theta(j)$ is 0 for negative j and 1 for positive j, $\theta(0)$ will be taken to be equal to $1/2$, according to equation (2.15). This is a result of the factor of two difference between powers of z in the expansion for f; this difference was discussed in reference to equation (2.9). Alternately, if we

recall that all δ functions should be assigned some nonzero width, then the above integral evaluates to 1/2.

4.2 Resummation

This theory exhibits a spontaneous breaking of circular symmetry. One starts the growth process with a circularly symmetric cluster, which implies that $G(j) = 0$ for $j > 0$, but this is not a stable state. Instead, the dynamics evolves G to one of an infinite number of states with nonzero $G(j)$, although on average $G(j) = 0$ for $j > 0$. If we impose some boundary condition, such as $G = 1$ at time $t = 0$, and look at G for much later times, the perturbation theory in a small noise term causes us to to reach large values of G. Having imposed these boundary conditions, the noise is amplified by the dynamics and will grow large.

This large growth of noise means that if we evaluate the two-point correlation function $\langle G(j)G^*(k)\rangle$ we will obtain some answer of the form $\delta(j-k)|G^2(j)|_{av}$, where $|G^2(j)|_{av}$ is an appropriate function of j, and $|G^2(j)|_{av}$ is much larger than $N(j)$. In the long time limit, $|G^2(j)|_{av}$ is not a function of time.

Then, we may imagine that, when calculating any other correlation function, at any stage in the perturbation theory, two lines which were contracted to obtain the value $N(j)$, can instead have their contraction dressed with additional interactions to convert $N(j)$ to $|G^2(j)|_{av}$. Two important points must be made about this procedure. First, it is important that this value $|G^2(j)|_{av}$ is completely uncorrelated with any other values of G in the diagram; all correlations are already taken into account by the interaction vertices of the diagram. Second, we must be careful to avoid overcounting; since each contraction in a diagram includes many diagrams involving dressing the contraction in various ways, we must not further dress these contractions.

For notational convenience, I will continue to write G^f everywhere, but now

$$\langle G^f(j)G^{f*}(k)\rangle = \delta(j-k)|G^2(j)|_{av} \tag{4.6}$$

G^f is similar to a free field in field theory. Any average product of several G^f can be decomposed into pairwise products. This is the resummation of noise into two-point correlation functions of G that was mentioned above in the comparison to Navier-Stokes perturbation theory. $G^f(j)$ is now an unknown function of j; one of the goals of the RG will be to determine the dependence of this function on j.

Similarly, the function $s(j)$ can be resummed. Any single line between two interaction vertices, which would normally be represented by a factor of $1/s$, will instead be represented by $1/s^{eff}$, where s^{eff} takes into account possibilities of dressing that line, without interactions with other lines. s^{eff} is an "effective" s. This is the resummation of propagators.

As a result of these two resummations, to avoid overcounting we must require that we do not count diagrams in which some portion of the diagram that contains interactions has only two lines leaving it. See Fig. 4 for examples of contributions to j, contributions to s^{eff}, and diagrams which can not be included in the theory as they would overcount contributions.

As one will be able to verify after performing the RG calculation, within the formal power series expansion of $(s + \frac{\partial}{\partial t})^{-1}$, one may neglect all terms in $\frac{\partial}{\partial t}$ in the RG calculation of the next chapter. Terms only flow to higher powers of $\frac{\partial}{\partial t}$. Because $|G^2(j)|_{av}$ is taken to be constant in time, terms with $\frac{\partial}{\partial t}$ will drop out in many places.

Then, the perturbation rules, ignoring time derivative, may be summarized as follows: draw all diagrams (subject to the rules forbidding overcounting), with appropriate external lines, assigning a factor of $1/s^{eff}(j)$ to each line, and a factor of $t(j,k)\theta(j-k)$ to each vertex, and a factor of $(s^{eff})^2(j)|G^2(j)|_{av}$ to each contraction on noise, while conserving momentum everywhere.

4.3 Example Calculation

It will be useful to give a simple example of applying such a perturbation theory to a non-interacting system. For example, consider the following simplified equation of

motion:

$$G_t(j) + sG(j) = t(j,j)G(j)G(0)G^*(0) + sG^f(j) \tag{4.7}$$

where $t(j,j)$ is proportional to $j - 2j - 1$ which is equal to $-j - 1$. Let us suppose G^f is constant in time, to simplify the problem further. Then, let us define the time scale so that $t(j,j) = -j - 1$. Let us pick the desired scale of the cluster so that $G(0) = 1$. Physically, $G(0)$ is very large compared to the noise $G^f(0)$. This mean that for a stationary state (after all, s is adjusted to produce a stationary average size) we may let $G^f(0)$ be small and we need s approximately equal to -1.

Now that the values of s, t are fixed, we may find the solution, either using perturbation theory or using a straightforward solution. The latter method gives $-G(j) = -G(j) - jG(j) - G^f(j)$. Therefore, $G(j) = G^f(j)/j$ and $\langle G(j)G^*(j)\rangle = N(j)/j^2$. This noninteracting system is stable.

The perturbation theory for $G(0)$ is slightly tricky. If we ignore the time derivative, we can only reach small values of $G(0)$ in the perturbation expansion. However, in fact, for the given s and t, a small $G^f(0)$ produces a large $G(0)$, under the time evolution. Let us suppose that this part of the process has been done, and that we obtain a resummed expression for $\langle G(0)G^*(0)\rangle$. This resummed expression is $|G^2(0)|_{av} = 1$. Then, we may ignore the time derivatives and obtain the expression for the higher $G(j)$ in a straightforward fashion.

The perturbation theory expansion to $G(j)$ gives the following infinite sum:

$$G(j) = G^f(j) + (|G^2(0)|_{av}t(j)/s)G^f(j) + (|G^2(0)|_{av}t(j)/s)^2G^f(j) + ... \tag{4.8}$$

This is equal to $G^f(j)(1-|G^2(0)|_{av}t(j)/s)^{-1} = G^f(j)/j$. This perturbation expansion is shown in Fig. 5. Each line terminates by setting G equal to the noise. Similarly, the perturbation expansion to the correlators gives a product of two infinite sums. This product is represented in diagrams by taking the sum in Fig. 5 and noise contracting it with its complex conjugate.

One may define $s^eff(j)$ for this simple theory; the diagrams of Fig. 5 define the

inverse of s^{eff}. Therefore

$$s^{eff}(j) = s - t(j)|G^2(0)|_{av} \tag{4.9}$$

which simplifies equation (4.8) to $G(j) = \frac{1}{s^{eff}(j)} sG^f(j)$.

Chapter 5

Renormalization Group Calculation

We investigate the effect of changing the cutoff in the equation of motion. This leads to the introduction of new diagrams to describe the changes in the theory as a result of lowering cutoff. It is shown how to incorporate these into a change in s, t. The fixed point is found.

5.1 Lowest Order Contributions to RG Flow

In the RG calculation, first the cutoff is lowered from Λ to $\Lambda - \delta\Lambda$. If the cutoff is imposed in a smooth fashion (interaction term $t(j,k)G(k)G(l)G^*(m)\exp[-(l+m)/\Lambda]$), the change in the theory under a change in the cutoff can be obtained by adding an additional term to the equation of motion (3.1), equivalent to the original cubic term, except that the cutoff $\exp[-(l+m)/\Lambda]$ is replaced by $(\delta\Lambda)\partial(\exp[-(l+m)/\Lambda])/\partial\Lambda$. This new term is

$$(1/\mu)\int dk\, t(j,k)\, G(k)\int\int dl\, dm\, G(l)G^*(m)(\delta\Lambda/\Lambda)(-(l+m)/\Lambda)\exp(-(l+m)/\Lambda) \times\delta(k+l-m-j)2\theta(j-k) \tag{5.1}$$

The sum of the original interaction term plus this new term is equal to the interaction term at reduced Λ. This term will have a circle around the vertex when it appears in a diagram.

Because this term is small when the external momenta l, m are small, it does not directly enter into correlation functions of the low momentum theory. It enters indirectly, in more complicated diagrams. We will then consider various such diagrams which include this term, and show that, for the simplest such diagrams, these diagrams may be rewritten in terms of a change in s and t.

This procedure has some slight logical differences with other RG procedures. In other procedures, the cutoff is often imposed in a sharp fashion at some momentum. Here, the cutoff is imposed in a very smooth fashion; I believe this has certain logical advantages. This procedure is similar to the technique of counterterms in the original formulation of renormalization in field theory.

First, I will evaluate the simplest diagrams to which this new term gives rise, and do the RG calculation, then in the next section I will consider other possible diagrams and explain why they are neglected. Throughout the RG calculation, when I write $|G^2(\Lambda)|_{av}$, I actually mean

$$\int dl \, |G^2(l)|_{av} \frac{\partial e^{-2l/\Lambda}}{\partial \Lambda} \tag{5.2}$$

This is just a weighted sum of $|G^2(l)|_{av}$ at l of order Λ, and due to the smooth cutoff it is this weighted sum that will enter into all the diagrams considered.

The diagrammatic expansion for s^{eff} will now include the diagram shown in Fig. 6. This changes $s^{eff}(j)$ to

$$s^{eff}(j) - t(j,j)|G^2(\Lambda)|_{av}\delta\Lambda/\mu \tag{5.3}$$

The term $2\theta(j-k)$ in equation (5.1) gives 1 in this case, as discussed in the perturbation theory rules.

Additionally, the new term in the equation of motion can give rise to a diagram as shown in Fig. 7a, which can be represented by changing $t(j,k)$. This arises from

substituting

$$s^{eff}(l)G(l) = G^f(m)t(l,m)G(n)G^*(o)\delta(m+n-l-o)2\theta(l-m) \tag{5.4}$$

and

$$G^*(m) = G^{f*}(m) \tag{5.5}$$

into equation (5.1), taking l of the order of Λ. The result changes $t(j,k)$ to

$$t(j,k) + 2(\delta\Lambda/\mu)t(j,k)t(\Lambda,\Lambda+k-j)|G^2(\Lambda+k-j)|_{av}/s^{eff} \tag{5.6}$$

Assuming Λ is high momentum and j,k are low momentum, then $\Lambda+k-j=m$ is high momentum. One does not use terms arising from substituting $s^{eff}(l)G(l) = G(n)t(l,n)G^f(m)G^*(o)$, instead of the substitution of equation (5.4), because such terms involve too many high momentum components of G. The diagram corresponding to this term is shown in Fig. 7b. Such terms should be ignored, as they will be small when determining the behavior of the system for momenta much less than Λ. Remember that the cutoff is imposed, in the original equation, on $G(l)$ and $G^*(m)$, not $G(k)$. This means that the presence of the high momentum term $G^*(m)$ will make such terms small.

All momenta are now rescaled by $\frac{\Lambda}{\Lambda-\delta\Lambda}$ to put the ultraviolet cutoff back at Λ. This changes $s^{eff}(j)$ to

$$s^{eff}(j) - j(ds^{eff}(j)/dj)(\delta\Lambda/\Lambda) \tag{5.7}$$

Because of the integration in the interaction term, and the one power of μ extracted from $t(j,k)$, the dimension of $t(j,k)$ is equal to (momentum)$^{-1}$. Therefore, under rescaling, the function $t(j,k)$ becomes

$$t(j,k) - j(\partial t(j,k)/\partial j)(\delta\Lambda/\Lambda) - k(\partial t(j,k)/\partial k)(\delta\Lambda/\Lambda) - t(j,k)(\delta\Lambda/\Lambda) \tag{5.8}$$

Combining the terms resulting from the integration, equation (5.6), with those

from the momentum rescaling, equation (5.8), every term in the change of $t(j,k)$ either is a function of $(j-k)$, or would be a function of $(j-k)$ if $t(j,k)$ were a function of $(j-k)$. For a stationary point, then require that

$$t(j,k) = t(j-k) \tag{5.9}$$

If $t(j,k) = t(j-k)$, then similar logic using equations (5.3),(5.7) requires that $s^{eff}(j)$ becomes a constant. These requirements of momentum independence of s,t likely do not hold at the extreme infrared for any true system, or else the equation of motion (equation (3.1) using renormalized t and s) would have no non-zero solution, but in the scaling region between the infrared and ultraviolet, they will hold.

For the rest of this section, the number s is the constant to which s^{eff} flows under the RG, and the number t is $t(0)$.

At this point, I have done the first part of the RG for the two numbers s and t. It is now necessary to rescale G to leave equation (3.1) invariant under the renormalization and rescaling. Let G be rescaled to

$$(1 - r(\delta\Lambda/\Lambda))G \tag{5.10}$$

This implies a rescaling of s to

$$(1 + r(\delta\Lambda/\Lambda))s \tag{5.11}$$

and a rescaling of t to

$$(1 + 3r(\delta\Lambda/\Lambda))t \tag{5.12}$$

Naively one might expect that there could also be an overall rescaling of both s and t by a factor a. This would leave G unchanged. Taking derivatives of $\log(s)$ and $\log(t)$ with respect to $\log(\mu)$ (since the ultraviolet cutoff is lowered to $\Lambda - \delta\Lambda$ and then rescaled back to Λ, it is actually μ that changes in this process), for s and t to

be stationary we find:

$$r - (\Lambda/\mu)t|G^2(\Lambda)|_{av}/s + a = 0 \tag{5.13}$$

$$3r + 2(\Lambda/\mu)t|G^2(\Lambda)|_{av}/s + a - 1 = 0 \tag{5.14}$$

This in itself does not provide enough information to extract anything useful, because having both r and a means that s and t can be scaled to arbitrary values.

5.2 Why $a = 0$

However, as will now be shown, $a = 0$. The freedom to take a non-zero a corresponds to a freedom to multiply the equation of motion (3.1) by a constant (neglecting the question of what happens when the noise is multiplied by such a constant). This is a general problem when renormalizing a classical equation of motion, instead of a field theory. For a field theory, the coefficient multiplying the action is of course very important.

In our problem, however, the renormalization takes place at the level of the diagrammatic expansion for the equation of motion, not at the level of the equation of motion itself. Consider a typical diagram of the theory. The propagators are assigned weight $1/s^{eff}$ and the noise contractions are assigned weight $s^{eff}G_f$. We could have arbitrarily redefined this to assign propagators the weight c/s^{eff} and to assign noise the weight $s^{eff}G_f/c$, where c is any constant. This would not change the theory. That is, there is not a one-to-one correspondence between the terms in the equation of motion and the diagrammatic expansion. Taking non-zero a would permit us to change the value of c.

However, when we renormalize s^{eff} as done in the previous section, this leads to a change in the weight we assign to a propagator having already picked a given value of c to determine the diagrammatic expansion. By requiring that at the fixed point the diagrammatic expansion remain unchanged, we require that $a = 0$.

Therefore, we may state that

$$a = 0 \tag{5.15}$$

5.3 Fixed Point

Then, the fixed point equations (5.13),(5.14) can be solved for

$$r = (\Lambda/\mu)t|G^2(\Lambda)|_{av}/s = 1/5 \tag{5.16}$$

This result for r is the main result of the first order RG.

This gives the rescaling of $G(j)$ with j. The magnitude of $G(j)$ must decay as $j^{-1/5}$. Thus

$$|G^2(j)|_{av} \propto j^{-2/5} \tag{5.17}$$

The combination $(\Lambda/\mu)t|G^2(\Lambda)|_{av}/s$ is invariant under a rescaling of G of G by equation (5.10) and a corresponding rescaling of s and t by equations (5.11),(5.12), and gives us the dimensionless coupling constant for this problem. From equation (5.16) the dimensionless coupling constant is $1/5$, which is not infinitesimal; however, after RG flow, the problem is no longer strongly coupled, as the constant is less than 1.

The reason that a factor of $1/\mu$ was removed from $t(j,k)$ is now clear; this makes the above coupling constant truly dimensionless. As a result of the removal of the factor of $1/\mu$, the dimension of $t(j,k)$ is (momentum)$^{-1}$. However, $|G^2(j)|_{av}$ has the dimension of momentum; this is because, taking G to be dimensionless, equation (4.6) gives $|G^2(j)|_{av}$ a dimension inversely proportional to the δ-function. The δ-function has dimension of inverse momentum, and thus the end result is to make $t|G^2(j)|_{av}$ dimensionless.

As a further comment on the dimensionality of the coupling constant, recall that the δ-functions have a finite height proportional to $1/\mu$. This finite height changes under the RG, which implies a rescaling of $|G^2(j)|_{av}$ under the RG flow; by multiplying t by $1/\mu$ we shift this rescaling onto t.

We may also say something about the magnitude of $G_t(j)$ for different j. The quantities sG and tG^3 remained constant under the RG, as a result of the rescalings of G, s, and t and the renormalizations of s and t, from equations (5.3),(5.6),(5.7),(5.8),(5.10). We also need G_t to remain constant since this is also a term in equation (3.1). Sup-

pose the characteristic inverse time scale for fluctuations in $G(j)$ is $\omega(j)$. Then $G_t(j)$ is of order $\omega(j)G(j)$. For this combination to remain constant, ω must change as a result of the rescaling of j in the RG. In fact, $\omega(j)$ must have the same log derivative under RG that s does, although the log derivative of s results from renormalization (equation 5.3) while the log derivative of $\omega(j)$ results from rescaling. This implies that

$$\omega(j) \propto j^{1/5} \tag{5.18}$$

This means that for smaller j, the time scale for fluctuations is longer. Returning to the original problem, as described by equation (2.29) with a time-dependent cutoff, this means that the lower Fourier coefficients grow at a roughly constant rate. This self-consistently justifies the adiabatic assumption of chapter 3.

5.4 Other Contributions to RG Flow

One may imagine that the new term of equation (5.1), representing the rescaling of the cutoff, may enter into additional diagrammatic contributions. Various possibilities are shown in Fig. 8. I will show that, for low momentum behavior, these terms are unimportant and then discuss in more generality why other contributions are negligible.

One may check by hand that the first example is small if external momenta are much less than Λ. The second example will be discussed below. The third example vanishes due to phase space factors. The fourth example vanishes due to phase space factors if the two lines leaving the top of the diagram are close in momentum; this means it does not alter the RG flow of $t(j,k)$ when $j = k$. In the rest of the section, various other diagrams will also be said to "vanish"; this will only mean that they vanish when considered either at low momentum or, if they contribute to the RG flow of $t(j,k)$, when considered at $j = k$.

The fifth example, a contribution to the six-point function, will be seen below to be small when calculating correlations of only 4, and not 6 or more, $G(j)$. The sixth example should not be considered when the rescaling of $|G^2(j)|_{av}$ is taken into

account; since $(\Lambda/\mu)|G^2(\Lambda)|_{av}$ is stationary under RG flow, such a diagram is canceled by the various rescalings.

In order to indicate in general why such contributions may be neglected, I would like to define some additional terminology to describe certain paths and contractions in these diagrams. When considering a contribution to s^{eff}, one may follow one line through the diagram as follows: start with the incoming line. At every t vertex, if one enters with $G(j)$, follow out along $G(k)$, not $G(l)$ or $G^*(m)$, where the roles of j, k, l, m are as in equation (3.1). If the line one is following is contracted (this will be referred to as an *exceptional contraction*) with a $G^*(m)$ leaving a t vertex, follow out along $G(l)$ of that t vertex. This path will be referred to as the *main line.* Now, any diagram that includes an exceptional contraction, such as the diagram of Fig. 8a, will be small for low momenta, since the $G(k)$ leaving such a diagram will only have a small range over which to integrate. For Fig. 8a the main line is given by following the horizontal arrow along the bottom of the diagram from left to right, through the t vertex, until it bends up and left. Then go down and left through the noise contraction into the t vertex, and then leave the t vertex along the line going up and left. Follow this line through its bend back to the right until it leaves the diagram.

The smallness, of the contribution to s^{eff} given in Fig. 8a, for small momenta does not completely justify the neglect of such terms. For example, when evaluating the RG contribution to t, the value of s^{eff} used is $s^{eff}(\Lambda)$, not the low momentum s^{eff}, and thus a high momentum contribution to s^{eff} may change the low momentum renormalized t. However, even for a calculation of $s^{eff}(\Lambda)$, the exceptional contraction will mean some reduction in available phase space over which to integrate.

One may check that contributions to $s^{eff}(j)$ like the third example in Fig. 8 will always vanish, regardless of what j is, due to the θ functions in equations (3.1),(5.1). The lines coming off of t vertices connected to the main line must be contracted within themselves, not between different vertices. In this diagram, the main line is simply the entire horizontal arrow running along the bottom of the diagram. Thus, the only contribution to s^{eff} will be the contribution of Fig. 6.

For contributions to $t(0)$, we may define 2 main lines. One can follow the main

line of the $G(l)$ or the main line of the $G^*(m)$. These are the lines one follows if one starts on the line for $G(l)$ or for $G^*(m)$ and follows through the various contractions as defined above. These two lines join at some point in a noise contraction.

The second example of Fig. 8 has an exceptional contraction and may be ignored. The main line starting with the $G(l)$ line leaving the circled t vertex proceeds up and left, then turns right, going straight across the diagram to the end. Then it turns down and left, up and left through an exceptional contraction into a t vertex. Then it goes down and left into a noise contraction, where it ends. The main line starting with $G^*(m)$ starts at the circled t vertex and proceeds up and right until it terminates at the noise contraction. Fig. 8b is very like Fig. 7b, except an additional t vertex has been added to the diagram. If this vertex were removed, this diagram would be small for small external momenta. With the t vertex on the diagram, the diagram is very difficult to evaluate since to evaluate it requires a knowledge of all $t(j,k)$, not just $t(\Lambda,\Lambda)$. However, the diagram is not only next order in the coupling constant, but also small due to the various exponentials present, as may be verified. Any diagram for t with such an exceptional contraction will have the same problems. That is why we will ignore them.

If the main line of the $G^*(m)$ has lines leaving it which contract against lines leaving the main line of $G(l)$ then the diagram will again vanish due to the θ functions. A contribution to t cannot have both external lines leaving the main line of $G^*(m)$. Therefore both lines must leave the main line of $G(l)$, and the line $G^*(m)$ cannot be dressed by any interaction vertices. Again due to θ-functions, the main line of $G(l)$ can only include one interaction vertex which has both external lines on it. For example, the diagram of Fig. 8d has external lines coming off different interaction vertices and vanishes if the two lines are close in momentum.

All that remains is to justify the neglect of six-, and higher-,point functions, such as could appear from the diagram in Fig. 8e. If we wish to calculate a correlation function of four $G(j)$, and somewhere in one diagrammatic calculation we have a six-point function, some of the lines leaving the six-point function must be contracted against each other. Then, somewhere in the diagram for the correlation is a contribution to

the four-point function which includes the six-point function within it. Therefore, the renormalization procedure would have yielded this contribution to the four-point function as a change in t. But, we have already, as outlined above, obtained all the contributions to the change in t. Therefore, there is no such diagram.

Finally, the lowest order contributions considered in the previous section have a certain universality; considering only the diagrams of that section, the nature of the fixed point does not depend on the initial form of $t(j,k)$. Higher order RG contributions will depend on the initial form of $t(j,k)$.

Chapter 6

Fractal Dimension and Multifractal Exponents

It is now possible to begin extracting exponents of the original DLA model. Different exponents correspond to different correlation functions of this model; it will be the purpose of this chapter to determine how to compute exponents from correlation functions. This process depends on the discussion of the adiabatic assumption and the assumption used to introduce the cutoff into the continuum equation. From those assumptions an unambiguous means of determining exponents from correlation functions is given.

In any actual simulation, there is an ultraviolet cutoff Λ determined by the ratio of macroscale to microscale. In the RG, a power law decay was found for $G(j)$. Since the RG describes a fixed point in the scaling region, within the RG itself this power law holds for arbitrarily large j. Within an actual simulation this power law will fail at j of order Λ, where Λ is the cutoff of equation (2.25) resulting from the finite size of the cluster in the simulation. Thus, in the calculation of exponents that follows, although all correlation functions are calculated using the rules of the RG and of perturbation theory, the integrals over correlations functions that we will use must be cutoff at momenta of order Λ, as will be done.

Since the size of the object follows a power law behavior given by

$$F_1 \propto t^{1/D} \tag{6.1}$$

where D is the radius of gyration dimensions of the object, we have

$$\frac{d\log(F_1)}{dt} \propto 1/t \tag{6.2}$$

As a side point, strictly speaking this requires that dF_1/dt can be replaced by the derivative of the average value of F_1, but both numerical evidence and the RG flow of frequency resulting from equation (5.18) justify this assumption. However,

$$dF_1/dt = \langle\lambda\rangle F_1 \tag{6.3}$$

where $\langle\lambda\rangle$ is defined to be the average value of λ over the unit circle at a given time. Equation (6.3) may be derived by using equation (2.14) to calculate dG_0/dt and then equation (2.26) to relate this to dF_1/dt. Combining equations (6.2),(6.3) we get

$$\langle\lambda\rangle \propto 1/t \tag{6.4}$$

Equation (6.4) is equivalent to the electrostatic scaling law first derived by Halsey[18, 19]. In the continuum approximation, $\langle\lambda\rangle = \int dj \langle G(j)G^*(j)\rangle$. Here it must be understood that while in the perturbation theory this expression is formally infinite, since $\langle G(j)G^*(j)\rangle = \delta(0)|G^2(j)|_{av}$, in the above average we remove this factor of $\delta(0)$[28]. Calling D the fractal dimension,

$$F_1^{-D} \propto 1/t \propto \langle\lambda\rangle \propto G_0^2 \int^{\Lambda} dj\, j^{-2/5} \propto F_1^{-2}\Lambda^{3/5} \propto F_1^{-2}F_1^{3/10} \tag{6.5}$$

This gives the result that

$$D = 2 - 1/2 + 1/5 = 1.7 \tag{6.6}$$

The first proportionality in equation (6.5) followed from the radius of gyration definition of the dimension. The second followed from the electrostatic scaling law. The third followed from the expression for $\langle\lambda\rangle$ in terms of G and from the scaling of G derived in the RG. The fourth followed from equation (2.26) and from doing the integral. The fifth followed from the functional dependence of Λ on F_1 as given by equation (2.25).

This is the simplest way to derive the fractal dimension from the above work. The calculation of the growth rate from equation (6.4) is essentially a determination of the unrenormalized, unrescaled s in equation (3.1). It may also be possible to repeat the same result by using the rescaling of s under the RG to obtain the rescaling of the growth rate under a shift in Λ.

The multifractal exponents $\tau(q)$ are defined by

$$\tau(q) = \lim_{l\to 0}\left(\log(\sum_i E^q(i))/\log(l)\right) \tag{6.7}$$

where the surface of the cluster is covered with intervals of length l, and $E^q(i)$ is the integral along the ith interval of the qth power of the electric field. Numerical calculations of these exponents can be found in references [24, 29].

One can try to compute higher multifractal exponents using the RG (the work above amounts to computing $\tau(3)$ and showing that $D = \tau(3)$). For example, the scaling of $\tau(5)$ can be determined by calculating the scaling of

$$\int^{\Lambda} dj\, dk\, dl\, dm\, \langle G(j)G(k)G^*(l)G^*(m)\rangle\delta(j+k-l-m) \tag{6.8}$$

against the upper cutoff Λ. This is because the given integral is equal to the desired power of the field integrated over the surface of the object. If all the terms in this integral contributed with the same phase, the integral would scale as $\Lambda^{-4/5+3}$. Of course, the terms are independent and this misestimates the exponent. It is necessary to use the perturbation theory to evaluate the 4 point correlation function. The simplest possibility is to use G^f as an estimate for all the G in equation (6.8). The

diagram for this is shown in Fig. 9a. The only terms that would then contribute would be when a G and a G^* were at the same momentum and the integral would scale as $\Lambda^{-4/5+2}$. The different scaling results from having a different number of momenta to integrate over. Another possibility (this is analogous to a tree approximation for a scattering problem) is to substitute for the highest momentum G in terms of a t vertex, leaving a six-point correlation function, and then take all six G, G^* to be G^f. The scaling is then as $\Lambda^{-6/5+3}$. The diagram for this is shown in Fig. 9b. Since this scales more strongly with Λ, it will be dominant in the limit needed to compute $\tau(q)$.

The following is the rule for calculating multifractal exponents:*Let n be a positive integer. Calculate the integral over 2n-point correlation functions defined by*

$$\int^\Lambda dj_1 \int^\Lambda dj_2 ... \int^\Lambda dj_n \int^\Lambda dk_1 \int^\Lambda dk_2 ... \int^\Lambda dk_n$$
$$\langle G(j_1)G(j_2)...G(j_n)G^*(k_1)G^*(k_2)...G^*(k_n)\rangle \delta(j_1 + j_2 + ... + j_n - k_1 - k_2 - ... - k_n) \tag{6.9}$$

If this integral behaves, in the limit of Λ taken to infinity, as Λ^a, where a is some number, then $\tau(2n+1) = (2n) - a/2$. The factor of $(2n)$ is the trivial scaling that would result even for a nonfractal object; the factor of $a/2$ results from the dependence on Λ and from the square root dependence of Λ on length scale.

In general, we can always find, for $\tau(q)$, a tree diagram that scales like $\Lambda^{-2(q-2)/5+(q-2)}$. Then,

$$\tau(q) = (q-1) - 1/2(-2(q-2)/5 + (q-2)) \tag{6.10}$$

Alternately, another definition of exponents is

$$D_q = \tau(q)/(q-1) \tag{6.11}$$

Then

$$D_q = \tau(q)/(q-1) = 1 - \frac{q(1/2 - 1/5) - 1 + 2/5}{(q-1)} \tag{6.12}$$

which is equivalent to

$$D_q = \frac{0.7q - 0.4}{q-1} \tag{6.13}$$

Chapter 7

Comparison With Numerics and Discussion

The theory is compared with numerics, and further tests of the theory are proposed.

7.1 Comparison With Numerics

In previous work we found that the alternate formulation of DLA using analytic functions[20] produces clusters with appearance and dimension similar to those of clusters grown using the lattice formulation of DLA. As far as we can tell, the two formulations are equivalent when $\alpha = 2$.

The simplest comparison with numerics is the dimension itself. 1.7 is very close to the accepted value of 1.71.

Equation (6.13) for higher multifractal exponents is the same as the formula obtained with a wedge model by Halsey et. al.[24], except that the wedge model left the quantities 0.7 and 0.4 as unknown constants to be fitted to numerics. They define quantities f and α, the dimension of the set on which the wedges exist, and the strength of the singularity (hopefully, the reuse of the symbol α will cause no confusion), and show that $D_q = \frac{\alpha q - f}{q-1}$. A numerical fit gave $\alpha = 0.705$, $f = 0.42$, while a comparison with equation (6.13) gives $\alpha = 0.7$, $f = 0.4$. It is now known that such a simple scaling law is not valid for large q[29], and in the original paper of Halsey et.

al. it was suspected that such a law would not hold.

The possible difference between theory and experiment here for large q should not be construed as a flaw in the presented work. First, the above calculation is only a lowest order calculation. To higher orders, we may find a form for $t(j,k)$ which has nontrivial behavior. This may alter the results from the tree approximation to the correlation function used to compute the exponents. Second, we may find interesting behavior if we consider other contributions to the correlation exponents, beyond the tree diagrams used above. Third, although the neglect of the appearance of 6-point function was valid when considering the renormalization flow of s and t, as discussed in reference to Fig. 8e, such a neglect is not valid if one actually wishes to compute 6- and higher point correlation functions. Fortunately, such multi-point interaction terms are captive variables, in the sense that if one knows the behavior of s,t under RG flow one may systematically determine the higher interaction terms that will appear. Fourth, the above derivation of multifractal exponents involved expressing the exponent in terms of correlation functions; this is only possible for odd multifractal exponents. Thus, in fact it is not possible to say anything about even exponents in any simple fashion.

Additionally, there exist some difficulties in numerical calculation of higher multifractal exponents. According to the branched growth theory of DLA [27], the time required to compute higher exponents is superexponential in the order of the desired exponent. Thus, the exact values of the larger exponents may not be precisely given by the numerical experiments. This mathematical difficulty may be the source of the controversy which appears to exist between the different numerical calculations of these exponents. For example, the value quoted for $\tau(3)$ by Ball et. al. is less than 1.6, which is definitely at odds with the electrostatic scaling law (believed to be exact from various numerical calculations), and with other numerical calculations of this exponent. The electrostatic scaling law says that $\tau(3) = D = 1.71$. There also exists controversy about the precise value of the dimension of DLA, as mentioned in Ref. [15]. Thus, in fact, it is not clear exactly how large is the discrepancy between the above results and the numerical results.

It is also of interest to numerically check the scaling of $G(j)$. This was checked for two cases. First, for a single cluster as described in the next paragraph; second, for an ensemble of clusters as described in the paragraph after that.

When $\int dj\, G(j)G^*(j)e^{-j/\Lambda}$ is plotted against $\Lambda^{0.6}$, where in reality the integral is a discrete sum, one expects to find a straight line behavior. This is what is found, as shown in Fig. 10, except that for large Λ the curve flattens out, since the numerical calculation only included a finite number of terms. Also for small Λ, the curve flattens out at F_1^{-2}, which, in the long time limit, is vanishingly small compared to the full integral. For the finite cluster size of our simulation, F_1^{-2} is not negligible. The clusters here were grown using the conformal mapping technique outlined previously. The coefficients of G were computed with a numerical Fourier transform, by mapping a large number of points on the surface of the circle (in fact, slightly outside the circle, to improve numerical behavior) to the surface of the aggregate (again, to slightly outside the surface of the aggregate) and analytically calculating the derivative of the mapping for each point. This technique is not very efficient for growing large clusters, at least as presently implemented. It requires $O(N^2)$ time to compute N growth steps, but it is very easy to calculate coefficients of G using this program. I only used aggregates of around 7000-10000 walkers.

As another check, 50 clusters of 6000 steps were simulated, and for each cluster, the coefficients of G were computed. The squares of these coefficients were scaled by $G(0)$, the overall inverse cluster size, and then averaged together. In Fig. 11 the mean squares of $G(j)$ are plotted against j on a log-log plot. Numerical difficulties made it impossible to accurately extract the slope in the scaling region. This scaling region extends from $j = 5$ to $j = 35$, or from $\log(j) = 1.6$ to $\log(j) = 3.5$. Theory predicts that this slope is $2/5 = 0.4$. The numerical slope is between 0.3 and 0.5, using a least squares fit. The theory line is drawn onto the graph. As an additional check, another ensemble of clusters was simulated, with a different λ_0 and a different number of steps. Within the scaling region of that simulation, the slope of the mean squares behaved in the same fashion, and, additionally, the mean-square of $G(j)$, after scaling by cluster size, for given j, was the statistically the same for the two simulations.

7.2 Discussion

A theory has been presented based on the conformal nature of various Laplacian growth processes. A series of approximations were made that produced a modified continuum equation of motion; it is hoped that such an equation describes DLA, but even if it does not, it does describe some form of nontrivial Laplacian growth. A perturbation theory was developed for this equation, and resummed. To determine various terms in the perturbation theory, it was then necessary to use a renormalization group calculation. This has only been carried out to lowest order. It is a peculiar feature of this method that next order calculations are vastly more difficult than lowest order calculations, thus as yet there is no analytic calculation of higher order effects. Finally, the assumptions leading to the modified model were reversed, leading to calculations of quantities for DLA.

It would be worthwhile to look more closely at higher order corrections, if not analytically, at least qualitatively, to see what may happen. To lowest order, $t(j-k)$ flows to an everywhere positive function. Using the lowest order t to compute the effect of higher order corrections will tend to lower the value for the dimension predicted by this theory. However, it is possible that in a more careful next order calculation, the interaction $t(j-k)$ flows to a function which is negative for large $(j-k)$, possibly increasing the predicted dimension. As mentioned above, next order effects depend in some way upon the initial functional form of $t(j,k)$. Lowest order effects do not.

Unfortunately, it is not possible to carry out a stability analysis of the fixed point of the lowest order RG. All that may be said from the above calculation is that if a fixed point exists, other than a trivial fixed point for which t goes to zero, then this fixed point is described by this RG.

It would also be worthwhile to try to extend this technique to other Laplacian growth models, such as the dielectric breakdown model. For the dielectric breakdown model[3], different values of η correspond, in the continuum limit, to different values of α in the conformal mapping model of chapter 2, section 1. The difference between

the dielectric breakdown model and our model is that, away from the DLA case, our model uses the same growth probability over the surface and varying walker size, while the dielectric breakdown uses a varying growth probability and constant walker size. Although this alters the scale of the cluster in our case, we would expect the fractal dimension of the cluster grown at a given α with the conformal model to be the same as the dimension obtained from the dielectric breakdown model with η equal to $\alpha - 1$.

One might naively try to apply the technique above to the case of α different from 2, by replacing equation (2.1) with the definition $G = F_z^{-\alpha/2}$, and using an equation of motion similar to (3.1), with different initial $t(j,k)$. This would lead to physically absurd results, and is in fact different from defining $G = F_z^{-1}$ and using a modified equation of motion as described in the next paragraph. The difference is in how the noise term is inserted. It is important for the perturbation theory that products of G^f may be pairwise decomposed, and this property means different things depending on whether $G = F_z^{-1}$ or $G = F_z^{-\alpha/2}$. In the stochastic problem, each growth step produces a simple pole of F_z^{-1} inside the unit circle; the angular coordinate of the pole is random, the radial coordinate is determined by λ. In the continuum limit of chapter 2, section 5, the angular coordinate becomes the real value of θ, while the radial coordinate becomes the imaginary value of θ; the interior of the unit circle is replaced by the lower half plane. One may show, using Cauchy's theorem, that randomly inserting *simple* poles produces a pairwise decomposition property for the random noise in F_z^{-1}. Therefore, the equation (2.1) is the best definition of G.

One *can* handle the case of α different from 2 by using a modified equation of motion, although this may be difficult if α is not even. One would modify equation (3.1) by including higher powers of G in the interaction term. For example, for $\alpha = 4$, the interaction term would be of the form

$$\begin{aligned}&(1/\mu) \int dk\, t(j,k) G(k) \int\int dl\, dm\, dn\, do\, G(l) G^*(m) G(n) G^*(o) \\ &\exp(-(l+m+n+o)/\Lambda) \delta(k+l+n-m-j-o) 2\theta(j-k)\end{aligned} \tag{7.1}$$

This would probably be the most worthwhile test of the calculations of this thesis;

although the calculation for $\alpha = 4$ is far more difficult than that for $\alpha = 2$, it may still be tractable to lowest order. It would not be appropriate to attempt such a calculation in this thesis. A few preliminary calculations show that one obtains at least the physically correct result that the dimension of the $\alpha = 4$ model is less than that of the $\alpha = 2$ model; as yet the exact value at $\alpha = 4$ is not calculated[30].

Appendix A

Figures

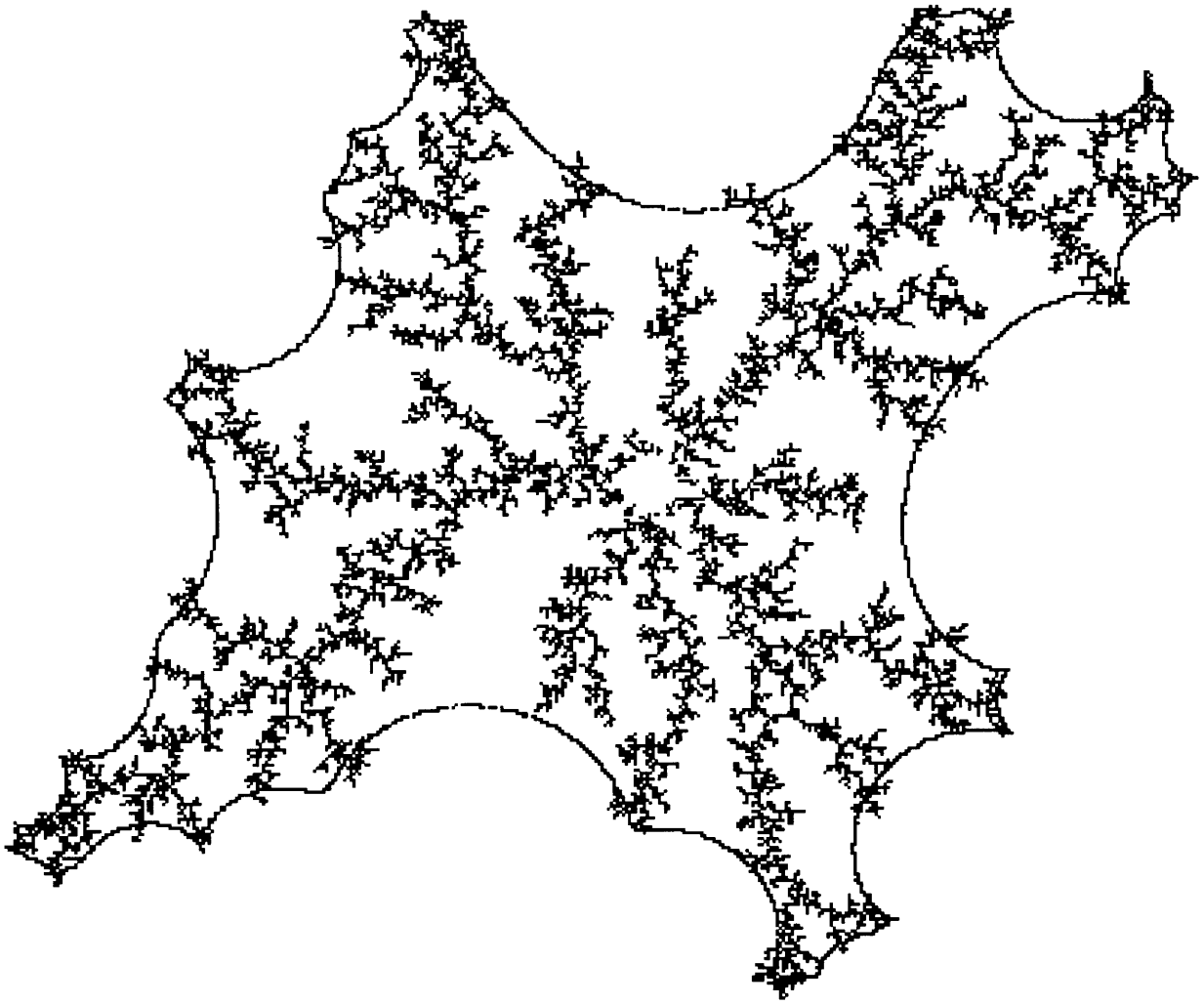

Figure A-1: Picture of a cluster grown using conformal growth model.

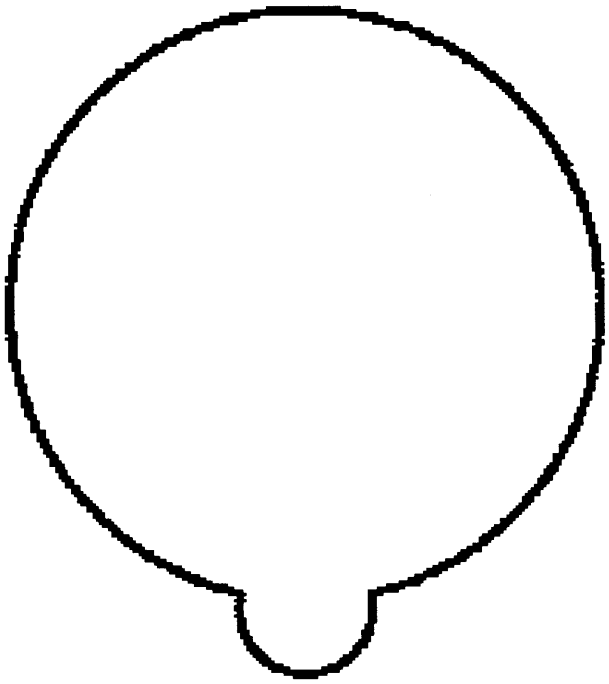

Figure A-2: Illustration of effect of f on the unit circle.

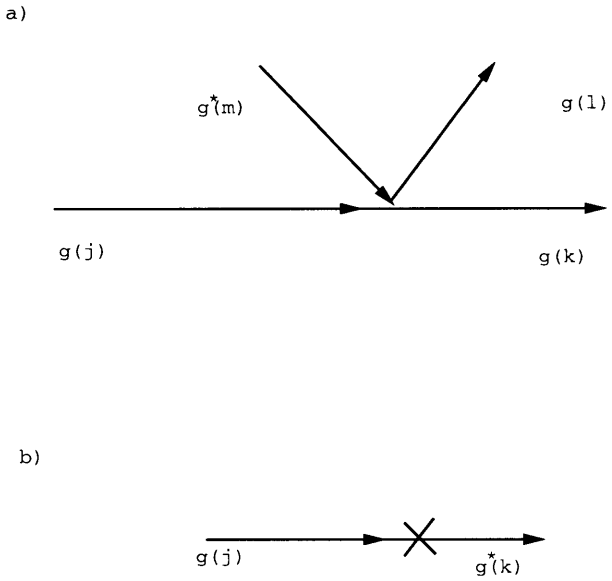

Figure A-3: Diagrams illustrating interaction vertex and contraction of noise terms. The first diagram results from setting $G(j) = \widehat{W}[j, G(k), G(l), G^*(m)]$. The second diagram would occur in evaluating $\langle G^f(j) G^{f*}(k) \rangle = \delta(j-k) N(j)$.

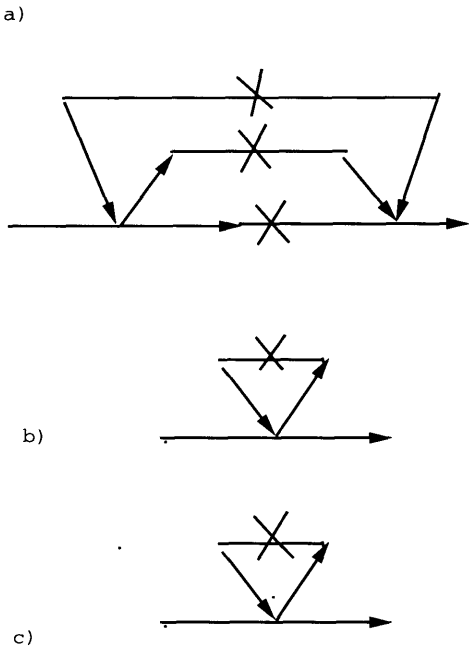

Figure A-4: a)A possible contribution to the average of $|G^2|$. b)A possible contribution to s^{eff}. c)A diagram which should not be considered if the propagators are already drawn in terms of s^{eff}.

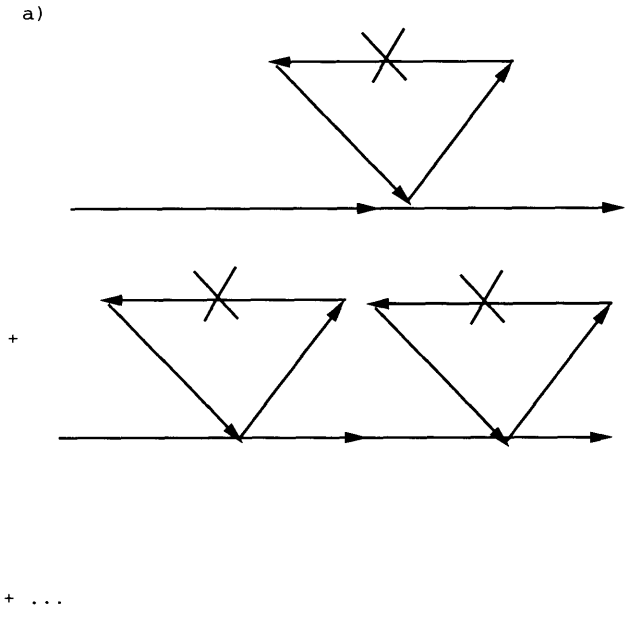

Figure A-5: Perturbation expansion in the example theory.

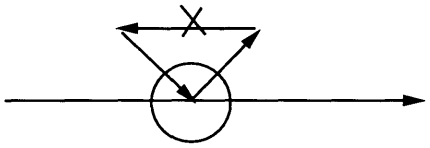

Figure A-6: Diagram contributing to the renormalization of s^{eff}.

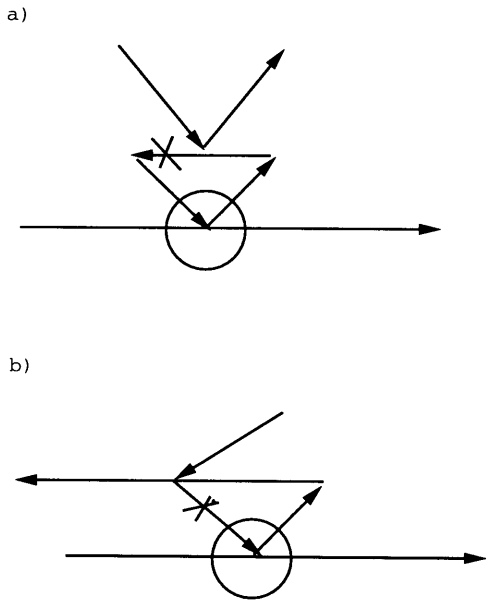

Figure A-7: a) Diagram contributing to the renormalization of t. b)Another possible contribution to the renormalization of t. This contribution is ignored. Certain difficulties are encountered in drawing this diagram. If the t interaction were drawn in standard form, many lines would need to cross each other.

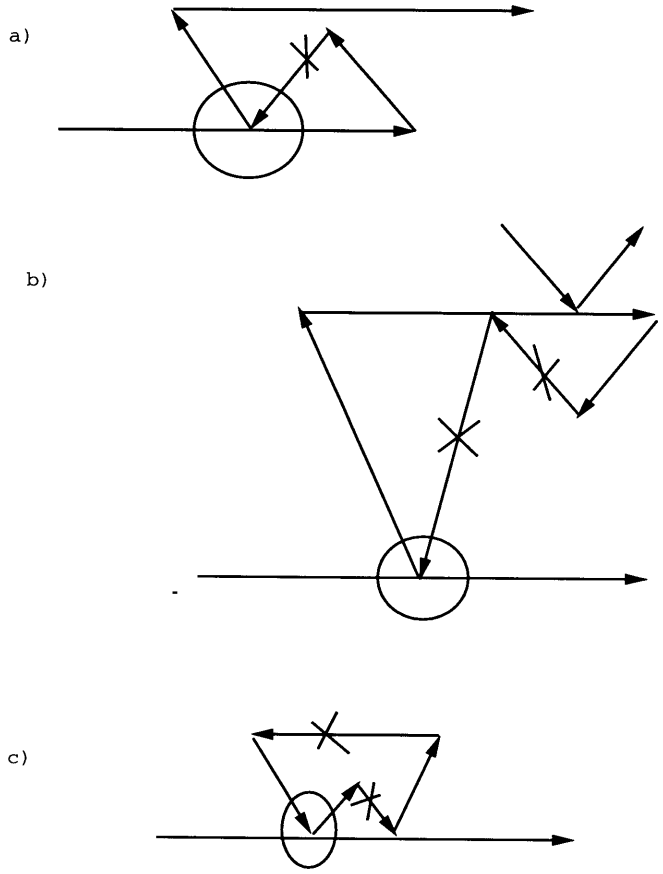

Figure A-8: Other possible contributions in the RG flow (a-c).

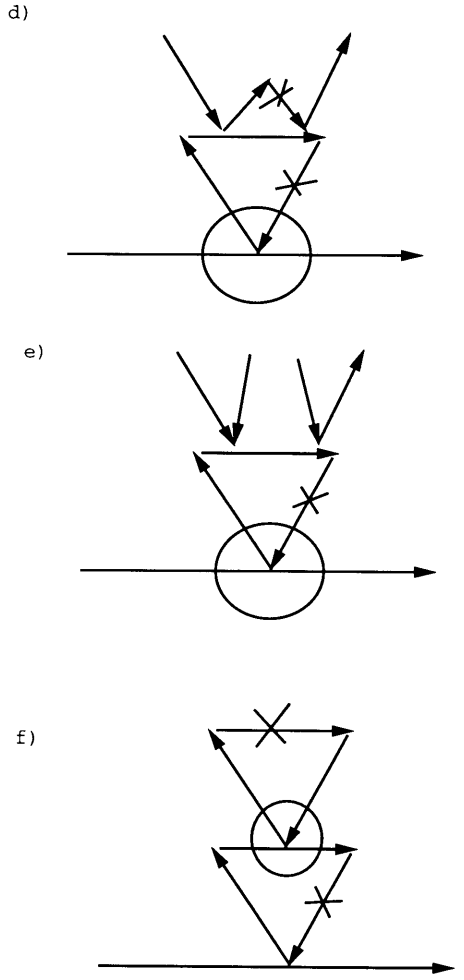

Figure A-8: Other possible contributions in the RG flow (d-f).

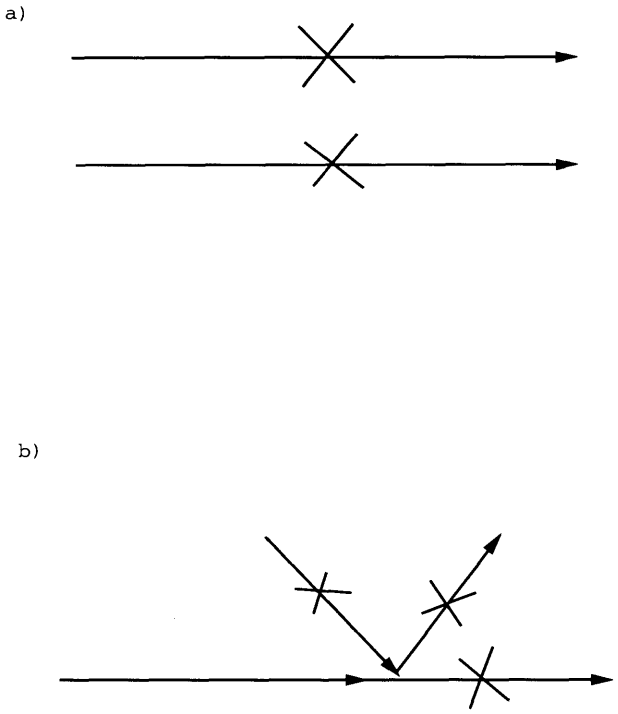

Figure A-9: a)Simplest diagram for the correlation function needed to compute $\tau(5)$. The external lines are the various $G(j), G^*(k)$ in the correlation function. b) Tree diagram for the same correlation function.

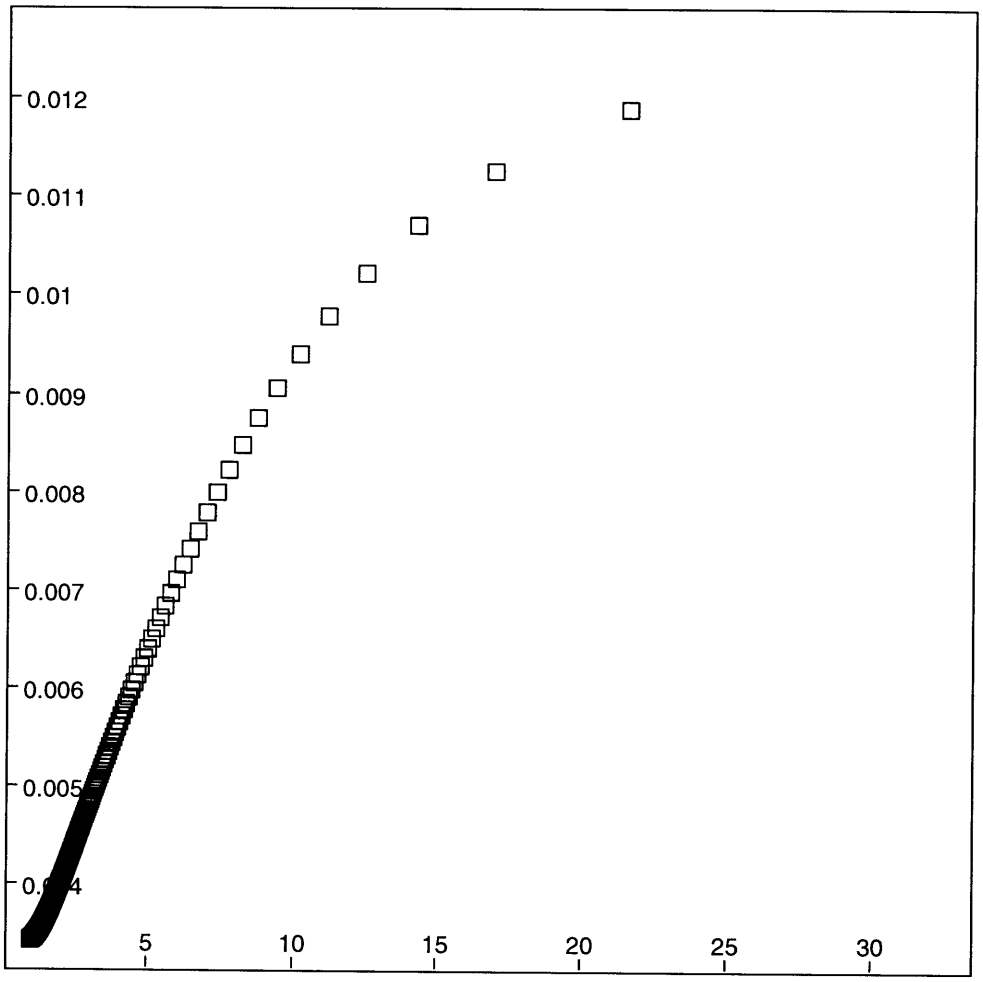

Figure A-10: Plot of scaling of λ against cutoff, as described in text.

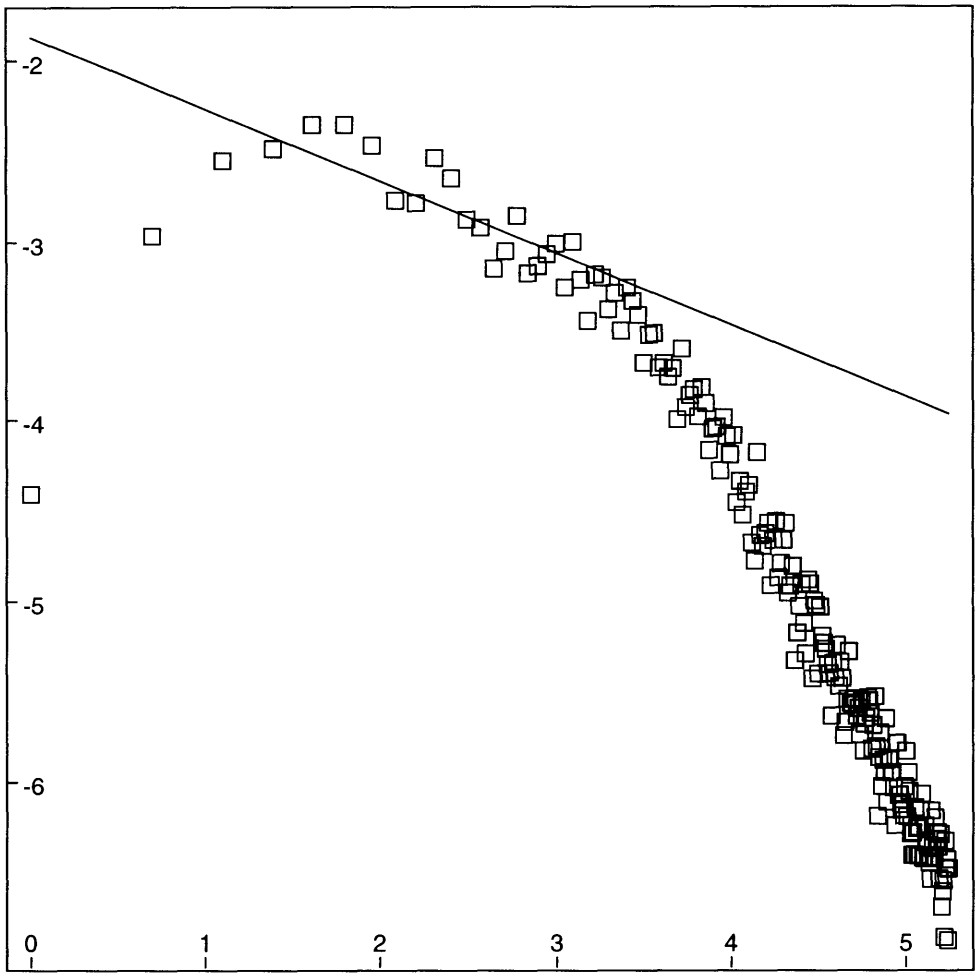

Figure A-11: Plot of scaling of log of mean square of $G(j)$ against log of j, as described in text.

Appendix B

Numerical Implementation of the Conformal Model

B.1 Discussion

This chapter describe the numerical implementation of the conformal model. There are two problems that must be solved in the numerical implementation. The first is how to store a representation of the function $F(z)$. The second is how to plot the cluster once it is grown.

The first problem is solved by storing, for each growth step, the given λ and θ for that growth step in an array (arrays *lj[]* and *theta[]* in the code below). Then, a function (*map()* in the code below) is used to map points by a conformal map $f(z)$ with given λ and θ. Finally, $F(z)$, for any given point z is obtained by iterating this map for each growth step. The local derivative of $F(z)$ is obtained by the chain rule.

The second problem at first might not seem to be a problem. Given a function $F(z)$ one can take a large number of points on the unit circle and apply $F(z)$ to each point. Unfortunately, the derivative of $F(z)$ is so large, and so wildly varying, that to obtain an accurate representation of the cluster would require a prohibitive number of points. This problem is solved as follows: the C program which implements the growth model picks a number of points on the unit circle by choosing them to be near the singularities of $F(z)$, and then outputs the mappings of these points. The

result is that the C program outputs a collection of points on the boundary of the cluster, giving a few points per growth step. When referring to singularities of $F(z)$, what is meant are either the zeroes of the derivative of $F(z)$ or the nearby square-root singularities of $F(z)$.

The C program which follows takes a number of arguments. The first argument is the number of growth steps. All arguments after that are optional and default to certain values if not entered. The second argument is a small number to control numerical error. This number measures the distance points are taken outside the circle before they are mapped with the conformal mapping. If this number is too small, there may be troubles with points being too close to singularities of the mapping. The third number is the value of λ_0. The fourth is the value of α. The fifth number controls the sharpness of the bump in the mapping. In general we replace equation (2.4) by

$$\left[\frac{1+\lambda}{2z}(z+1)\left(z+1+\sqrt{z^2+1-2z\frac{1-\lambda}{1+\lambda}}\right)-1\right]^a z^{1-a} \tag{B.1}$$

where a is the value of the fifth argument to the program. It is found that, so long as a is less than 1, the precise value of a does not matter. The case of $a = 1$ corresponds to "strike-mappings" as discussed in [20]. The sixth argument is a seed for the random number generator.

The program produces two files as output. The first file, "out", contains the logs of the values of λ for each growth step. The second file, "outhp", contains five numbers on each line. The first two numbers are coordinates of points in the plane. The third number indicates to which other point that point connects. By plotting a line between these two points, one obtain a picture of the cluster.

The last two numbers are not necessary for plotting and simply help keep track the topology of the branching. The first number of these two indicates how many branches connect the given point to the circle. The second number of these two keeps track of at which growth step the given point was produced; it is non-zero for one point in each growth step.

B.2 C Code

```
#include <math.h>
#include <stdio.h>
#define pi              3.14159

#define Npixel          3120
#define nmax            55000
#define frk            12000
#define true 1
#define false 0
static double prec;
typedef unsigned char boolean;
static double x[nmax],y[nmax];
static double cs[frk];
static long ref[nmax];
static boolean vtype[nmax];
static long ind[frk];
static int circ[nmax];
static int A, B, i, n, k, k1, i1, i2, j1_, j2, ipoint, j, m, klow;
static double lambda, lambda0, x1, x2, y1_, y2, r, theta[nmax],
ctheta, stheta, scale, c1;
static double lj[nmax];static double apow;
static char s[256], ordered[256];
static FILE *Fwr;
static int branch;
static int age[nmax];
static int root[nmax];
static double map(cj)
int cj;
```

```
{
  double u, v, a, b, c, d, r1, r2;
  double q,r,s,t,o,p,r3,jacoby,c2,d2;
  double ct;double lr,ar;
  u = x[i - 1] * ctheta + y[i - 1] * stheta;
  v = y[i - 1] * ctheta - x[i - 1] * stheta;
  if (u*u+v*v<1) {a=sqrt(u*u+v*v); u=u/a; v=v/a;}
  if (ref[i - 1] == i && u > (1 - lambda) / (1 + lambda)) {
    if (u * u + v * v > 1.01) {
      printf("tbad i=%3ld\n", i);
      /*geTS(s);*/
    }
    cs[m - 1] = u;
    ind[m - 1] = i;
    m++;
  }
  a = u * u - v * v + 1 - 2 * u * (1 - lambda) / (1 + lambda);
  b = 2 * u * v - 2 * v * (1 - lambda) / (1 + lambda);
  r1 = sqrt(0.5 * (sqrt(a * a + b * b) + a));
  r2 = b / (2 * r1);
  /*figure out whether to use r or minus r*/
  /*figure out where branch cut is*/
  ct=(1-lambda)/(1+lambda);
  ct=u-ct;
  if (fabs(ct)>fabs(v))
  {if (ct<0) {r1 = -r1; r2 = -r2;}}
  else
  {if ((r2*v)<0) {r1 = -r1; r2 = -r2;}}
  c = u + 1 + r1;
  d = v + r2;
```

```
  a = 0.5 * (1 + lambda) * ((u + 1) * c - v * d) / (u * u + v * v);
  b = 0.5 * (1 + lambda) * ((u + 1) * d + v * c) / (u * u + v * v);
  c2 = a * u + b * v - 1;
  d2 = b * u - a * v;
lr=log(c2*c2+d2*d2)*apow+log(u*u+v*v)*(1-apow);lr=lr/2;
ar=atan2(d2,c2)*apow+atan2(v,u)*(1-apow);
c2=exp(lr)*cos(ar);
d2=exp(lr)*sin(ar);
    x[i - 1] = c2 * ctheta - d2 * stheta;
    y[i - 1] = d2 * ctheta + c2 * stheta;
  if (cj)
  {/*calculate jacobian*/
  s=u+u*u-v*v;
  t=v+2*u*v;
  o=(u-(1-lambda)/(1+lambda))*r1+v*r2;
  p=r1*v-r2*(u-(1-lambda)/(1+lambda));
  r3=r1*r1+r2*r2;
  o=o/r3;
  p=p/r3;
  o=o+1;
  q=s*o-t*p;
  r=s*p+t*o;
  s=q-c;
  t=r-d;
  s=s*(1+lambda)/2;
  t=t*(1+lambda)/2;
  r3=(u*u+v*v); r3=r3*r3;
  s=s/r3;
  t=t/r3;
  o=s*(u*u-v*v)+t*(2*u*v);
```

```
  p=t*(u*u-v*v)-s*(2*u*v);
 o=apow*o;
 p=apow*p;
 lr=log(u*u+v*v)*(1-apow)+log(c2*c2+d2*d2)*(apow-1);
 lr=lr/2;
 ar=atan2(d2,c2)*(apow-1)+atan2(v,u)*(1-apow);
 a=exp(lr)*cos(ar);
 b=exp(lr)*sin(ar);
 s=o*a-p*b;
 t=o*b+p*a;
 lr=log(u*u+v*v)*(0-apow)+log(c2*c2+d2*d2)*(apow);
 lr=lr/2;
 ar=atan2(d2,c2)*(apow)+atan2(v,u)*(0-apow);
 o=exp(lr)*cos(ar)*(1-apow);
 p=exp(lr)*sin(ar)*(1-apow);
 o=o+s;
 p=p+t;

  jacoby=sqrt(o*o+p*p);}
     return(jacoby);
}

main(argc, argv)
int argc;
char *argv[];
{double l2;double alpha;FILE *q;
  long FORLIM1;int scl;int i2;
 int fd[2];int jj;long seed;
q=fopen("out","w");
lambda=0.005;scl=0;alpha=1;prec=0.00000001;apow=1;
```

```
branch=atoi(argv[1]); if (argc>=3) prec=atof(argv[2]);
if (argc>=4) lambda=atof(argv[3]);
if (argc>=5) alpha=atof(argv[4]);
if (argc>=6) apow=atof(argv[5]);
if (argc==7) seed=atoi(argv[6]);
l2=lambda;
  Fwr = NULL;
  srand((unsigned int)seed);
  n = 1;
  for (i = 1; i <= nmax; i++)
    vtype[i - 1] = true;
i=1;
  for (j = branch; j >= 0; j--) {
theta[j]=((double)rand())/pow((double)2,(double)15);
    theta[j] = 2 * pi * theta[j];
   /*calculate lj[j]*/
   lj[j]=l2;
  i2=j+1;
 x[i-1]=(1+prec)*cos(theta[j]+prec);
 y[i-1]=(1+prec)*sin(theta[j]+prec);
  while(i2<=branch) {
 ctheta=cos(theta[i2]); stheta=sin(theta[i2]);
 ref[i-1]=10;lambda=lj[i2];
 lj[j]=lj[j]/pow(map(1),alpha);
i2=i2+1;}
fprintf(q,"%lg %ld\n",log(lj[j]),branch-j);
}for (i=1;i<=nmax;i++) circ[i-1]=0;
n=0;
for (j=0;j<=branch;j++)
{ n++;
```

```
    lambda=lj[j];
    ctheta = cos(theta[j]);
    stheta = sin(theta[j]);
    if (n < nmax) {
      x[n - 1] = (1+prec) * cos(theta[j] + prec);
      y[n - 1] = (1+prec) * sin(theta[j] + prec);
      ref[n - 1] = n;
      age[n-1]=0;
      root[n-1]=n+1;
      m = 1;
      FORLIM1 = n;
      for (i = 1; i <= FORLIM1; i++)
map(0);
      m--;
      /****** order the array cs[m] ********/
      do {
strcpy(ordered, "true");
FORLIM1 = m;
for (k = 1; k <= FORLIM1; k++) {
  if (k < m) {
    if (cs[k - 1] > cs[k]) {
      c1 = cs[k - 1];
      k1 = ind[k - 1];
      cs[k - 1] = cs[k];
      ind[k - 1] = ind[k];
      cs[k] = c1;
      ind[k] = k1;
      strcpy(ordered, "false");
    }
  }
```

```
}
      } while (strcmp(ordered, "true"));
      /************** ready ****************/
      n++;
      x[n - 1] = (1+prec) * cos(theta[j] + prec);
      y[n - 1] = (1+prec) * sin(theta[j] + prec);
      ref[n - 1] = n;
      circ[n-1]=branch+1-j;
      age[n-1]=0;
      root[n-1]=n;
      ipoint = n;
      FORLIM1 = m;
      for (k = 1; k <= FORLIM1; k++) {
ref[n + k - 1] = ipoint;
vtype[n + k - 1] = false;
k1 = ind[k - 1];
        for (jj=1;jj<n-1;jj++)
        if (root[jj-1]==k1) {root[jj-1]=n; age[jj-1]+=1;}
if (k1 != ref[k1 - 1]) {
  printf("tno good%3ld%3ld\n", m, k);
}
x[n + k - 1] = 0.5 * (x[ipoint - 1] + x[k1 - 1]);
y[n + k - 1] = 0.5 * (y[ipoint - 1] + y[k1 - 1]);
        root[n+k-1]=n;  age[n+k-1]=1;
        ref[k1 - 1] = n + k;age[k1-1]=1;
ipoint = k1;
      }
      n += m;
    }
  }  /*branch*/
```

```
  /************* ready *****************/
  /************* plot ready ***************/
  strcpy(s,"outhp");
Fwr=fopen(s,"w");
  fprintf(Fwr, "lambda= %10.6f\n", lambda);
  FORLIM1 = n;
   for (i=0;i<n;i++)
fprintf(Fwr," %lg %lg %ld %ld %ld\n",
x[i],y[i],ref[i]-1,age[i],circ[i]);

 fclose(q);
  if (Fwr != NULL)
    fclose(Fwr);
  exit(0);
}
```

Appendix C

Numerical Results at Varying Values of α

C.1 $\alpha < 1$

For $\alpha < 1$, the growing cluster is always macroscopically stable. It has the form of a circle when viewed on a large scale. Similarly, we find that the coefficients in the power series expansion for $F(z)$ are all small compared to the first term F_1. The value of this first term can be written in closed form:

$$F_1 = \prod_{0<j\leq n} (1 + \lambda_j) \tag{C.1}$$

where n is the number of growth steps, and λ_j is the value of λ at the j-th growth step.

If the object were perfectly circlar, λ_j would be determined solely by the value F_1 before the j-th growth step. This would lead to a power law behavior of F_1 like

$$F_1 = (1 + \alpha\lambda_0 n)^{1/\alpha} . \tag{C.2}$$

It is found numerically that noise in the higher coefficients of the power series leads to

some renormalization of $\lambda_0 \to \tilde{\lambda}_0$, and then we obtain instead the power law behavior

$$F_1 = \left(1 + \alpha\tilde{\lambda}_0 n\right)^{1/\alpha}. \tag{C.3}$$

C.2 Phase Transition

As function of α, there is a transition at $\alpha = 1$ from stable to turbulent growth. The stable growth at $\alpha < 1$ is similar for the strike (parameter a discussed in Appendix B set equal to 1) and the bump models(parameter a discussed in Appendix B set less than 1): the degree of roughness of the cluster boundary, scaled in the cluster size, decreases with time.

The transition was analyzed numerically in the strip geometry. This is growth of the cluster in a periodic strip of contant width, instead of the circular or upper-half plane geometries considered elsewhere. The reason for choosing the strip geometry was that, after a certain amount of time has elapsed, for given λ_0, the boundary of the cluster is statistically unchanging. The magnitudes of all Fourier components stay roughly constant in time. Compare this to the circular geometry in which the the object becomes more and more finely detailed, with higher and higher Fourier components contributing to the shape of the boundary.

Then, for various values of α both greater and less than 1, the magnitude of the surface roughness (measured by the mean square of F_{-1} in equation (C.4) below), was numerically determined for various values of λ_0. It was found that for $\alpha < 1$, as λ_0 decreases, the surface roughness also decreased, presumably going to zero as λ_0 goes to 0. At $\alpha = 1$, there was a large jump in the surface roughness, and decreasing the value of λ_0 did not affect the madnitude of the roughness. The numerical results may be found in [20].

One may easily understand this phase transition by a simple analytical argument. Writing down a power series expansion for F in the strip geometry in analogy with

that for the circular geometry, one obtains:

$$F(z) = z + F_0 + F_{-1}e^{iz} + F_{-2}e^{2iz} + ... \tag{C.4}$$

where the mapping is defined for $\mathrm{Im}(z) > 0$ and the mapping is periodic when z is replaced by $z+2\pi$. If one then converts the continuum equation of motion appropriate to the given value of α to the strip geometry, and linearizes the resulting non-linear equation about small values of F_{-k}, one obtains the result that for $k > 0$

$$\dot{F}_{-k} = k(\alpha - 1)F_{-k} \tag{C.5}$$

Then, for $\alpha < 1$, the linear equation of motion is stable, while for $\alpha > 1$, the linear equation of motion is unstable.

C.3 $\alpha > 1$

The turbulent growth at $\alpha > 1$ is sensitive to the model. In the strike-models the object grows by emanating long chains of strikes (macro-strikes), which contain almost all the density at $\alpha > 1$.

For all bump-models at $\alpha > 1$ we find macroscopically unstable growth, with a power law growth rate, with some power greater than $1/\alpha$. For the bump-models, at $\alpha > 1$ the growing object forms a self-similar fractal cluster, with the fractal dimension varying with α. The self-similarity was checked by calculating gyration radius, which is found to be a power law function of time, and by calculating fractal dimension using the box counting method. The box counting fractal dimension was slightly lower, but was consistent with the gyration radius power law. The difference is most likely due to the small sample size (approximately 10000 steps). The cluster grown at $\alpha = 2$ has properties identical to that of a DLA cluster. This is expected, since at $\alpha = 2$ the new object size remains roughly constant throughout the growth. So, the $\alpha = 2$ bump models are equivalent to DLA. At other values of $\alpha > 1$, a relationship between the conformal model and the dielectric breakdown model at $\eta = \alpha - 1$ is

conjectured, but there are no numerical results as yet.

Bibliography

[1] B. B. Mandelbrot, The Fractal Geometry of Nature (Freeman, San Francisco, 1982); B. B. Mandelbrot, Fractals: Form, Chance and Dimension (Freeman, San Francisco, 1977).

[2] M. Eden, in Proc. 4-th Berkeley Symposium of Mathematics, Statistics, and Probability, Ed. F. Neyman (University of California Press, Berkeley, 1961).

[3] L. Niemeyer, L. Pietronero, and H.J. Wiesmann, Phys. Rev. Lett. **52**, 1033 (1984).

[4] M. Kold, R. Botet, and R. Juillien, Phys. Rev. Lett. **51**, 1123 (1983); P. Meakin, Phys. Rev. Lett. **51**, 1119(1983).

[5] T. A. Witten, Jr. and L.M. Sander, Phys. Rev. Lett. **47**, 1400 (1981).

[6] F. Hausdorff, Mathematische Annalen **79**, 157 (1919).

[7] A. S. Besicovitch, Mathematische Annalen **110**, 321 (1935).

[8] One may find a list of fractal and topological dimensions for a number of sets in the back of reference[1].

[9] A. Erzan, L. Pietronero, A. Vespignani, Rev. Mod. Phys. **67**, 545 (1995).

[10] H. G. E. Hentschel and I. Procaccia, Physica (Amsterdam) **8D**, 835 (1983)

[11] I. Procaccia, Phys. Scr. **T9**, 40 (1985)

[12] P. Meakin, H. E. Stanley, A. Coniglio, and T. A. Witten, Phys. Rev. A **32**, 2364 (1985).

[13] Tokuyama, M. and Kawasaki, K., Phys. Lett. **100A**, 337 (1984)

[14] Honda, K., Toyoki, H., and Matsushita, M., J. Phys. Soc. Jpn. **55**, 707 (1986).

[15] This result is the accepted result from many radius of gyration calculations. A lower result for the surface dimension is claimed by F. Argoul, A. Arneodo, G. Grasseau, and H. Swinney, Phys. Rev. Lett. **61**, 2558 (1988). Also see G. Li, L. M. Sander, P. Meaking, Phys. Rev. Lett **63**, 1322 (C) (1989).

[16] B. B. Mandelbrot, talk at 1997 APS March Meeting.

[17] T. C. Halsey, Phys. Rev. Lett **72**, 1228 (1994).

[18] T. C. Halsey, Phys. Rev. Lett. **59**, 2067 (1987)

[19] T. C. Halsey, Phys. Rev. A **38**, 4789 (1988).

[20] M. B. Hastings and L. S. Levitov, cond-mat/9607021

[21] M.B. Mineev-Weinstein and R. Mainieri, Phys. Rev. Lett. **72**, 880(1994).

[22] B. Shraiman and D. Bensimon, Phys. Rev. A**30**, 2840 (1984).

[23] Z. Nehari, Conformal Mapping, Chap.V, Sect.4, (Dover, N.Y., 1975).

[24] T. C. Halsey, P. Meakin, and I. Procaccia, Phys. Rev. Lett. **56**, 854 (1986).

[25] H. W. Wyld Jr., Ann. Phys. **14**, 143 (1961)

[26] D. Forster, D. R. Nelson, M. J. Stephen, Phys. Rev. A **16**, 732 (1977).

[27] T. C. Halsey, K. Honda, B. Duplantier, to be published.

[28] Actually, $\delta(0)$ is of order $1/\mu$, and so this formal infinity is quite correct. When integrating the electric field over the circle, the result should be proportional to the size of the circle. From the point of view of the continuum limit of section 2.5, this size is infinite, but in reality it is cut off at size $1/\mu$.

[29] Various authors have calculated these exponents. For example, R. C. Ball, O. Rath Spivak, J. Phys. A **23**, 5295 (1990) and references therein; C. Armitrano, Phys. Rev. A **39**, 6618 (1989).

[30] For $\alpha \neq 2$, equation (2.20) gets replaced by $\mathrm{Re}(F_t \frac{|F_z|}{zF_z}) = |F_z|^{1-\alpha} - \alpha|F_z|^{2-\alpha}\epsilon\mathrm{Re}(\frac{zF_{zz}}{F_z|F_z|})$ and so the balancing of electric field and surface tension of equation (2.23) is at the same value of ϵ. It is expected then, that equation (2.25) is that appropriate equation for any value of α. We found from equation (2.20) that $\delta = \epsilon$. Since δ is the distance of the zero of F_z to the boundary of the unit circle, and $R \propto 1/\delta^2$, this suggests that equation (2.25) may have a geometrical explanation, as well as a dynamical explanation.